BBCI

Technische
Universität
Berlin

COGNITIVE WORKLOAD IN THE MARITIME ENVIRONMENT

THE MARIN EXPERIMENTS

K+S projects

MARIN

PHILIPS

Contents

1 Introduction

The human factor plays the key role for safety in many industrial and civil every-day operations in our technologized world. Human failure is more likely to cause accidents than technical failure, e.g. in the dangerous job of tugboat captains. Here, cognitive workload is crucial, as its excess is a main cause of dangerous situations and accidents while being highly subject and situation dependent. However, reliable subjective ratings are hard to obtain while objective ratings of task difficulty remain a necessity for training as well as control, port and operation design – leading to a very high general interest in online cognitive workload indicators.

2 Contributions

Within this project we have conducted a simulator pilot study involving 10 professional tugboat captains and a variety of physiological measurements. We were involved in the design of the study, while we also played a key role in the execution of the experiments. We have linked the different measurements with the simulator data to enable a thorough analysis of interactions and influences. Within the experiments, we have supplied and set up most of the measurement equipment, conducted the technical maintenance and supervision of the physiological measurements as well as the generation and operation of a special side-task inducing cognitive workload. Also, we have been in charge of the whole data collection. In the data analysis, our main part was the extraction of the relevant markers for the different experimental conditions and the EEG analysis.

On the physiological side we recorded a 64channel high quality Electroencephalogram (EEG) with active electrolyte gel contacted electrodes in an extended 10-10 position set. With the same amplifier system we recorded an Electrocardiogram (ECG) of the heart in a standard 3 electrode montage optimized for R-peak detection. Also, the breathing activity of the subjects was assessed with a special piezo-driven belt.

2.1 Workpackages

All workpackages mentioned in the contract have been complied with:

- Concept for concurrent EEG acquisition in a manoeuvring simulator [**preparation of pilot study I; in discussions with partners**]
- Elaboration of an experimental design in consideration of EEG acquisition and validation [**preparation of pilot studies I and II; in discussion with partners**]
- Detailed analysis of the neural correlates of workload changes [**see this report**]
- Development of a tailored workload classifier and evaluation of its performance [**see this report**]

as well as three visits to MARIN:

- Visit 1: discuss experimental setup in manoevring simulator; 1 day [**done on 24.04**]
- Visit 2: implement EEG acquisition and supervise execution of first experiments; 4-5 days [**done 28.06. - 03.07.: pilot study I**]
- Visit 3: continuation of experiments, if required with a change of the experimental paradigm; 3-4 days [**done 11.09. - 18.09.: pilot study II**]

3 Project Description

3.1 Background

In the maritime world, as in many other workplaces, working memory, the ability to process information and to take decision are crucial. The quantification of *cognitive workload* is a measure to study these aspects. The insight can shed light onto the limitations posed by the *human factor* and point out how to improve equipment, conditions or the training for dealing with challenging tasks. While there exists no generally accepted definition of cognitive workload, there is a large agreement that it encompasses the two concepts of *activation* and *resources* or capacity.

In the present study, as we break new ground in the study of workload in the maritime world, we concentrated as a first step just on the net effect. A finer grained analysis including a distinction of different underlying factors, which can be expected to lead to enhanced system performance in the long run, is left as a topic for future research.

3.2 Neurophysilogical Correlates of Cognitive Workload

Cognitive workload is reflected in different components of brain activity. In view of the present target application, modulations of event-related potentials due to workload ([18, 19, 25]) are not relevant, since there are no controlled and continuously repeated stimuli. Therefore, we concentrate on workload-induced modulations of spontaneous brain activity.

The power of oscillatory brain activity in the theta frequency range (4 to 7 Hz) in frontal brain regions have been found to positively correlate with the level of workload, see e.g. [11, 13, 29].

With respect to the more prominent alpha frequency band, most studies report a negative correlation of cognitive workload and alpha power at parito-occipital scalp locations, see e.g. [10, 13]. However, these studies used tasks in the visual modality to induce workload, such that one can only derive the implication of alpha reduction for workload in visual resources. In general, the functional role of alpha band oscillations is not yet conclusive. For a memory task in the auditory domain, [12] reports a modulation of theta osciallations only, but no modulations of the alpha rhythm. Some studies using auditory stimulation even found an increase of alpha activity with increasing workload ([8, 17, 20, 22]). A possible interpretation is provided by the hypothesis of functional inhibition, which postulates that strong alpha activity reflects active inhibition of task-irrelevant processes ([16]): when the critical processsing load is in the non-visual, the visual areas are actively deactivated.

The idea of build EEG-based workload monitoring systems was presented, e.g. in [9, 10, 23, 26, 27]. On online system was built by our group and validate during an actual driving task on a highway ([3, 17]).

3.3 Performed Experimental Studies

As foreseen in the project proposal, two pilot studies have been conducted. The first study was conducted from June 30th to July 3rd with four participants. It was an important experience and the evaluation of this dataset underlined the viability of neurophysiological workload measurements in a manoevering simulator. The analyses have been circulated and discussed bwteen the project partners and resulted in small but important changes in the experimental setting for the follow-up study. Here, we will only report the results of the revised, second study which included ten participants.

3.4 Experimental Design

In a 10-subject simulator study, we recorded electroencephalographic data from a realistic tugboat scenario with professional captains (subj. 8 excl.: sickness). The experiment consisted of 3 different scenarios (approx. 40 mins each), where scenario 1 and 3 were identical, see Fig. 1.

While in scenario 1 and 3, the cognitive workload was modulated by the sailing task itself, we increased it in scenario 2 by an additional task (2-back task [15]) and kept sailing constant. The blocks were subdivided into epochs of 1 min for classification for all conditions.

3.4.1 Scenario 1&3: Bow-To-Bow

In this scenario the focus was to keep the experimental conditions as naturalistic as possible while still being able to modulate the workload induced on the captain. Therefore, 3 conditions were generated with different tasks and different weather conditions.

Condition 1: Free Sailing Condition: *low workload*: The captain was instructed to follow a large container ship astern while the weather was manipulated to have no extra effect on the workload.

Condition 2: Connecting Condition: *high1 workload*: After moving to the front of the vessel the tugboat captain gets the instruction to get ready for bow-to-bow connection while the weather conditions get harsh. He is told to wait for connection for 5 mins.

Condition 3: Pulling Condition: *high2 workload*: After the rope is connected, a constant tow force and line length is instructed while the weather stays harsh.

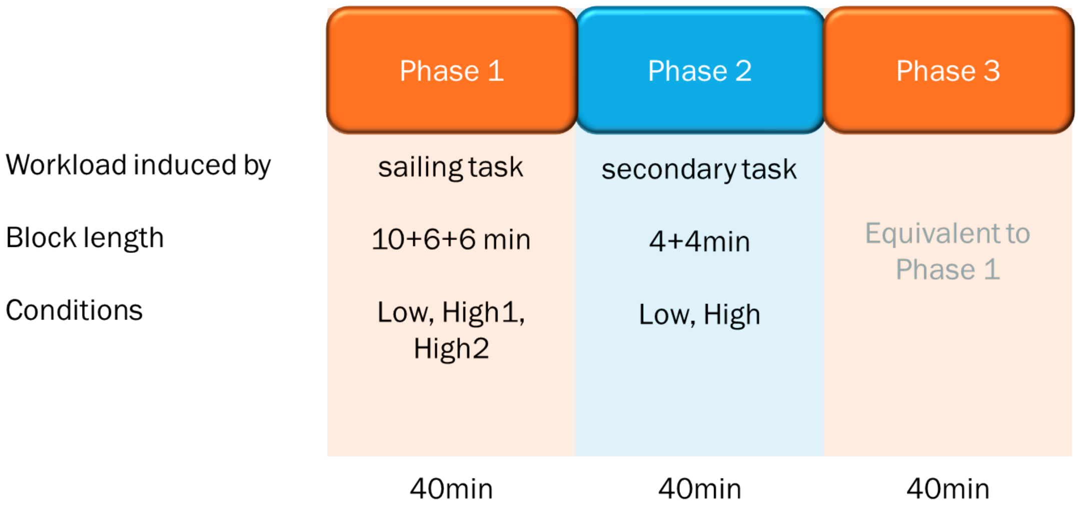

Figure 1: Experimental Design

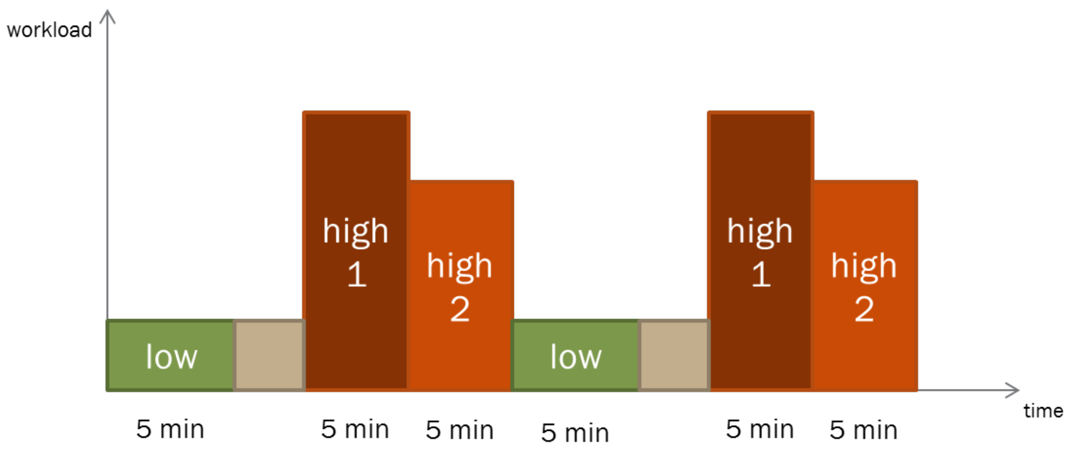

Figure 2: Experimental Design - Bow-To-Bow Scenario

3.4.2 Scenario 2: n-Back

The *n-back task* is commonly used in neuroscientific research as a manipulation tool for cognitive workload, where n is typically chosen between 0 and 3 in order to induce different levels of workload. We used this to have a condition comparable to common research and to see how much our bow-to-bow scenario corresponds to the neural patterns of this commonly known task. We used a auditory 2-back task, where the subject had to follow a stream of spoken numbers. If the last number heard corresponded with the digit 2 back, he had to press a button. The digits 1-9 were used with 3 s interleave randomly (75%) and forced 2-back repetition (25%) to get a reasonable amount of repetitions. The 2-back was played auditorily to keep a realistic behavioral scheme of the captain. There were 2 conditions, 4 mins each:

Condition 1: Free Sailing Condition *low workload*: In this condition, the same low workload task of the bow-to-bow Scenario is induced for comparison.

Condition 2: Free Sailing with 2-Back Condition *high workload*: The 2-back task was used additionally to the Free Sailing to induce a higher workload while keeping the primary task constant.

Both conditions were repeated 5 times resulting in a total duration of 40 minutes for the whole phase.

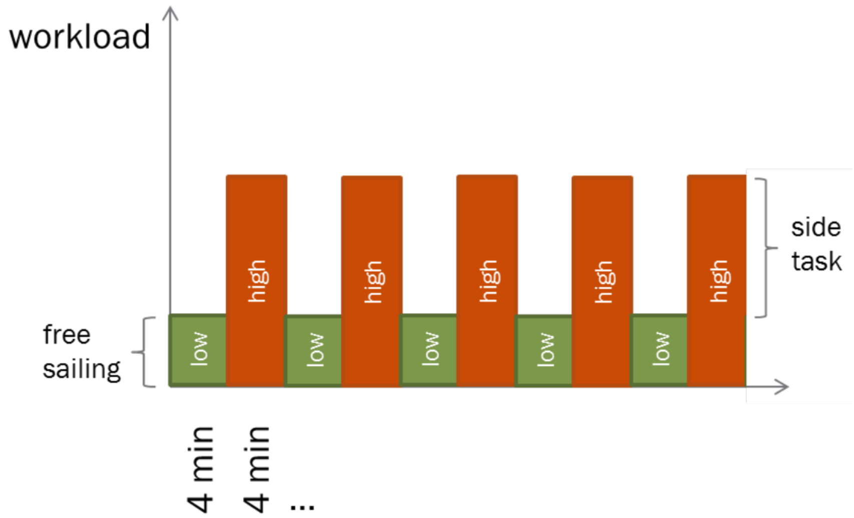

Figure 3: Experimental Design - n-Back Scenario

4 EEG-Analysis

4.1 Dealing with Artifacts

A preliminary analysis of the spatio-spectral content of the data showed that the EEG of some participants is heavily affected by artifacts. This was expected due to the participants being allowed to act naturally. Head and trunk movements were required for the sailing tasks, as the simulator provided a 360° projection.

First the automatic artifact removal method MARA ([31]) has been employed, that gives good results in usual EEG datasets. The method is based on a decomposition of the multivariate EEG by the use of an Independent Component Analysis (ICA; [1, 5, 14]). The components are classified into artifacts and neuronal components. Then, the cleaned EEG signals are obtained by projected only the neuronal components back into the sensor space. The classifier that distinguishes between artifactual and neuronal components was trained on a large data based of EEG datasets for which the ICA decomposition was manually annotated. For datasets that contain artifacts unlike those ones contained in the training data base, some of the artifactual components may go undetected. This seems to be the case for the dataset at hand.

Therefore, we went the tedious way of annotating all ICA components (ICs) manually. This decision between artifactual and neuronal components is based on the following plots: the propagation pattern that corresponds to the IC, the time series of the IC and its power spectral density. The number of components that are to be checked equals the number of EEG channels, i.e. 32 for the first three participants and 64 for the remaining seven. Examples of those plots are given in Figures 4, 5 and 6.

4.2 Results

The grand average (i.e., average across participants) of the spectral analysis is shown in Figure 7 (2-back task) and Figure 8 (bow-to-bow task). Corresponding plots for single participants are provided in appendices A and B. When comparing the results for individual participants, it becomes clear that the grand average is only of limited use. The effect of the workload conditions seen in the alpha band varies with respect to the specific frequency range (lower or higher alpha).

The most informative plot are the scalp maps of the r^2 scaled difference of high minus low workload condition, which are at the bottom of the figure. The four maps correspond to the four intervals that are shaded in the plot of the power spectral density. There is one for the theta range, two for alpha and one for beta.

In the grand average for the *auditory 2-back task* (Fig. 7, we observe a weak fronto-central increase in the theta band. However, we expect that this is not the typical theta effect, since its location is not as frontal as expected and the difference gets stronger in the frequency range below the theta band. (A typical frontal increase of theta activity can be seen for participant #10 in the bow-to-bow condition, see the last plot in Appendix B.) In the alpha range at 11 Hz, the power *increases* for the workload condition at parietal site (focus at Pz). This effect is opposite to generally assumed one of alpha decrease,

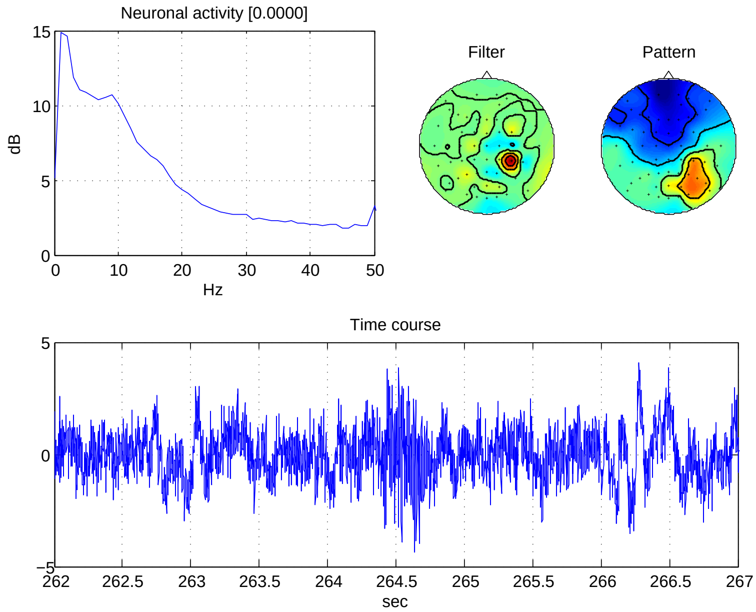

Figure 4: Inspection of a component obtained by ICA (neuronal component). The pattern (upper right subplot) gives an idea of where the activity originates from, in this case it is presumably the motor area corresponding to the left arm. The pattern shows a smooth dipolar structure. The power spectral density graph (upper left subplot) shows the typical $1/f$ shape with enhanced power around 9.5 Hz, which is the typical frequency of the sensorimotor rhythm. The time course does not display obvious irregularities.

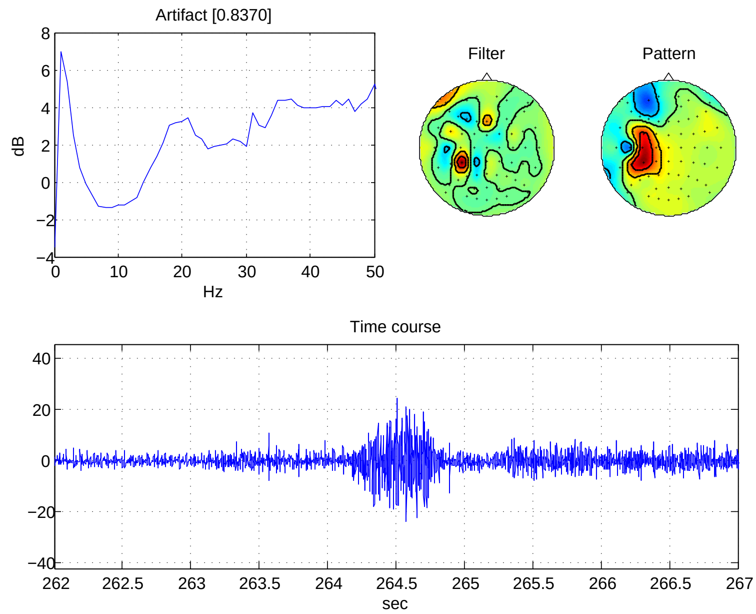

Figure 5: Inspection of a component obtained by ICA (artifactual component). Pattern, spectrum and time course do not look like neuronal activity: the pattern is very focal, the spectrum does not follow the general $1/f$ shape, has least power in the 10 Hz range and strong power in high frequencies and the time course contains a burst of high frequencies.

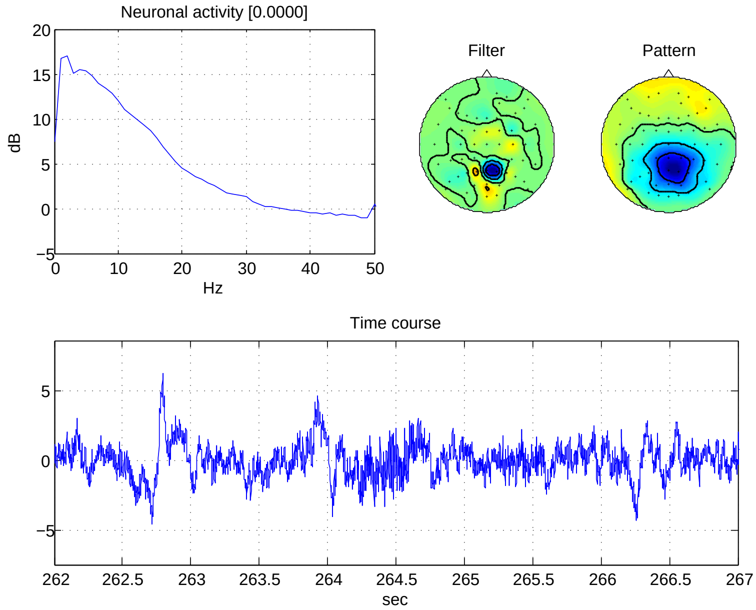

Figure 6: Inspection of a component obtained by ICA (neuronal component). Pattern, spectrum and time course look like neuronal activity: The pattern has a smooth monopolar structure and the spectrum follows the $1/f$ shape with a small increase in the theta frqeuency range.

which is based on studies with visual tasks but consistent with some studies employing auditory tasks, see Sec. 3.2. It is worth to notice that the frequency that shows the pronounced difference between the workload condition does not coincide with the alpha peak in the spectrum. In the plots for the single participants, this increase in alpha activity is visible in 6 out of 8 participants, while one (VP #3) shows the opposite effect (parieto-occipital alpha decrease) and the last one (VP #10) displays no clear effect (alpha decrease with wide spread parietal extend).

In the grand average of *bow-to-bow* scenario, the differences are much weaker (note the different scale). The lower alpha range shows an increase in power for high workload which looks topographically similar to the effect found in the *2-back* task. However, here the frequency showing the difference is below 10 Hz, which suggest that a different neural mechanism is observed here. In the plots for the single participants, this alpha modulation is visible for 4 out of 8.

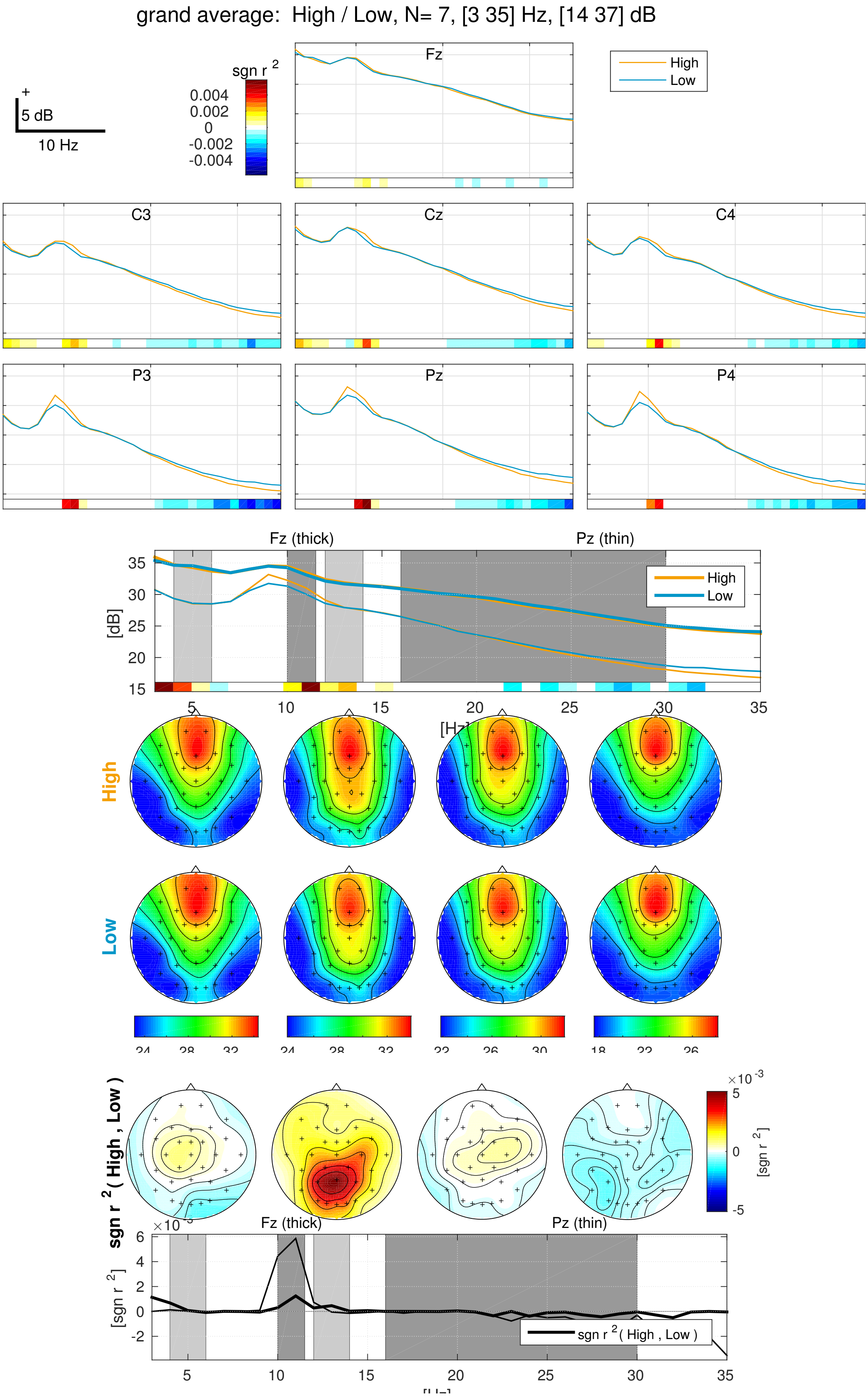

Figure 7: Grand average of the spectral analysis of the 2-back task.

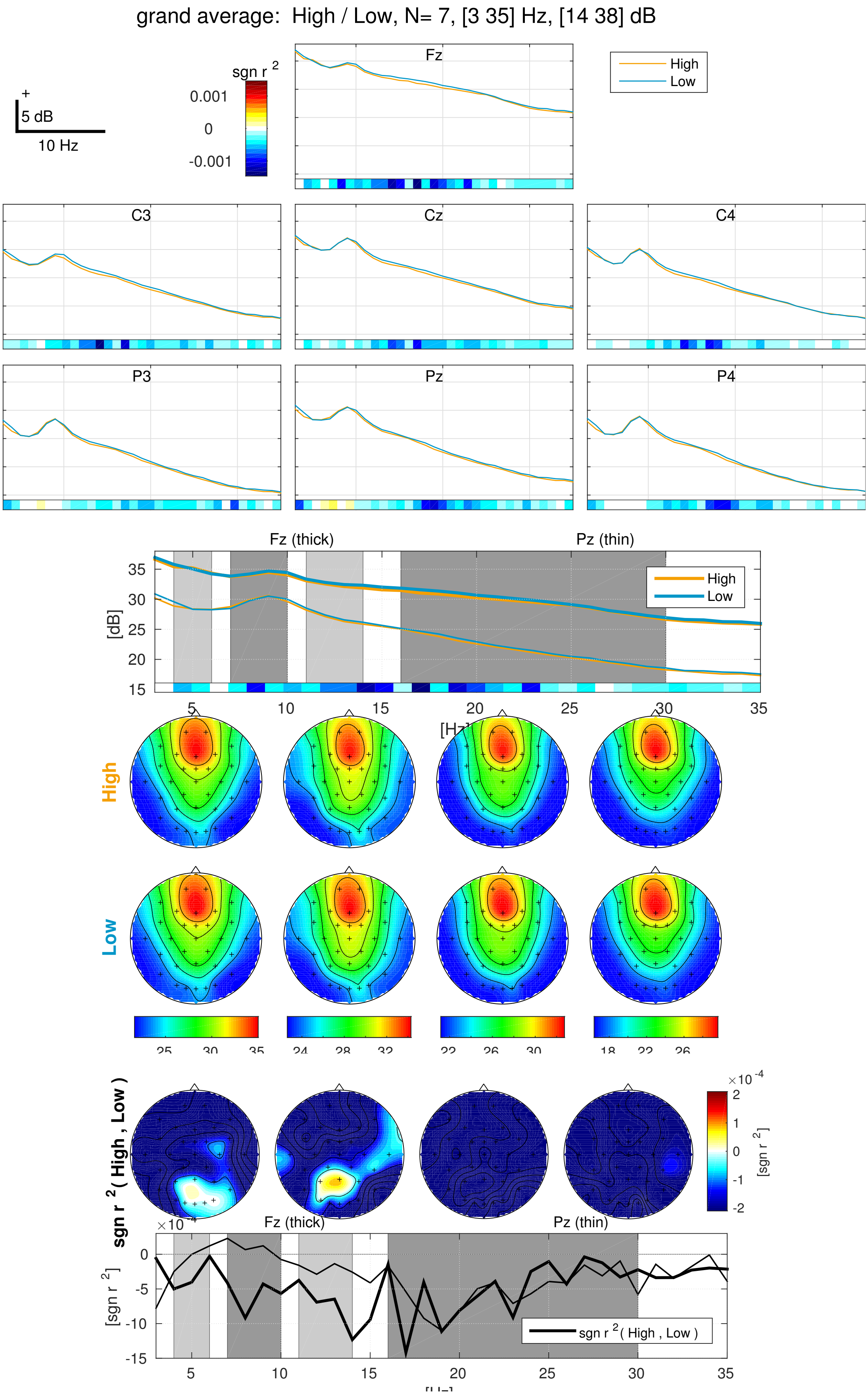

Figure 8: Grand average of the spectral analysis of the bow-to-bow task.

5 Classification Analysis

5.1 Aim and Approach

We have seen in the spectral analysis, that the data is strongly affected by artifacts. Apart from noise of the technical devices, there are artifacts from muscle activity (seen in high frequencies, mostly at outer temporal and occipital electrodes) as well as from eye movements (seen in low frequencies at very frontal channels). Furthermore, there may be motion artifacts due to the motion of the electrode cables induces by head and trunk movements.

The muscular and ocular artifacts are indicative of the workload condition for a number of participants and could in principle be used for the workload classifier. However, the goal of this analysis was to estimate the contribution of genuine brain activity to the estimation of the workload level. We did not design a classification method that specifically uses those artifacts. Still, we evaluated an approach that works on uncorrected data, we can be expected to exploit workload-specific artifacts to some degree, and methods including artifact corrected data which work presumably on brain activity only.

5.2 Preprocessing, Artifact Reduction and Feature Extraction

We used 1 Hz high-pass filtering alone (R), in combination with MARA [31] (C), an Independent Component Analysis (ICA, [1,5,14]) based automatic artifact reduction, as well as manual ICA artifact reduction (CM), as mentioned above. Then, we built different spectral band power based features based on windows of 60 s: (a) 1 Hz bins from 1–20 Hz, (b) 1 Hz bins from 4–12 Hz, **c** sum over alpha (8–12 Hz) and theta band (4–7 Hz) bins, and (d) sum over alpha (8–12 Hz), theta band (4–7 Hz) and beta band (13–20 Hz). In addition, we performed Common Spatial Pattern analysis (CSP; [7], for application in BCI context see [4, 24, 28]) in different band combinations [2] with the logarithm of the variances as features [4]. We evaluated the different classification designs within phases as block-wise cross-validations (CV; see [21] conerning the issue with validating blockwise data) as well as between phases to test for generalization. The CSP analysis was performed on the training set only and transferred to the test set, cf. [21].

5.3 Classification

The classifier was based on regularized linear discriminant analysis ([6]) with automatic shrinkage of the covariance matrix ([30]) after the different preprocessing steps.

5.4 Results

The results show a high variability in performance between participants. Classification works best in the *2-back scenario* (phase 2), but also the intra-phase classification in the more complex *bow-to-bow* scenario (phases 1 and 3) works quite well with CV-loss below 25 % for methods **R** and **C**. The transfer of the classifier between the different kinds of tasks (*2-back* and *bow-to-bow*) yielded results around the chance level, while the transfer of classifiers within the *bow-to-bow* scenario, i.e. between phases 1 and 3, works almost as good as the respective within phase classification (compare upper and lower subplot of columns 1 and 3 of Figure 9).

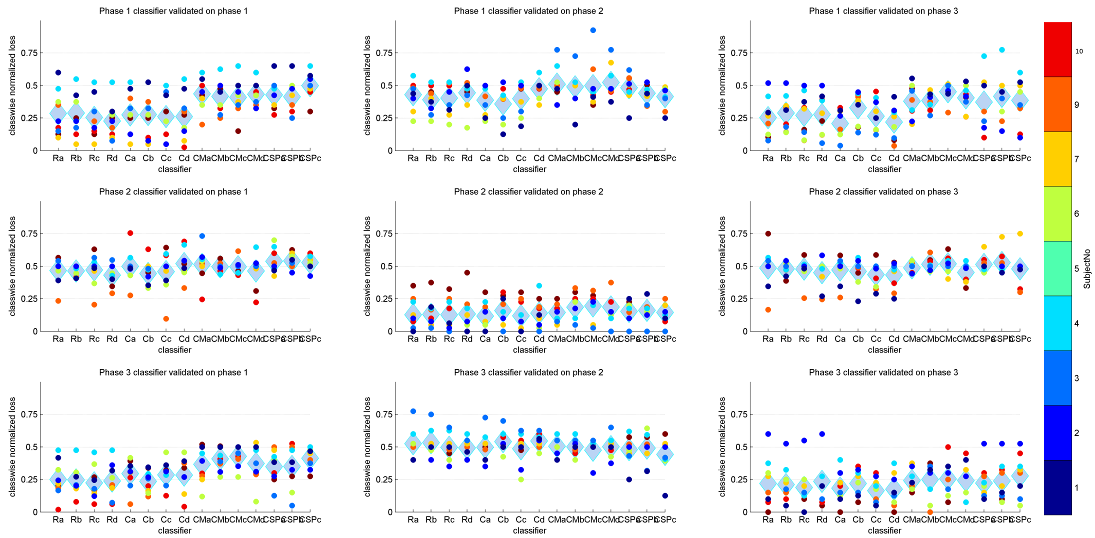

Figure 9: Classification Results: class wise normalized loss. The average classification result is indicated by the light blue marker, while the results for individual participants are shown as colored circles. Methods are labelled by capital letters for preprocessing and lower-case for different combinations of frequency bands: **R** only high-pass (1Hz), **C** MARA artifact removal, **CM** manual ICA based artifact removal: **a** 1 Hz bins from 1–20 Hz, **b** 1 Hz bins from 4–12 Hz, **c** sum over alpha (8–12 Hz) and theta band (4–7 Hz) and **d** sum over alpha (8–12 Hz), theta band (4–7 Hz) and beta band (13–20 Hz). CSP common spatial pattern algorithm: **CSPa** alpha and theta band, **CSPb** alpha, beta and theta band and **CSPc** alpha, beta, gamma and theta band.

6 Discussion

The results of the *2-back* scenario already show the complexity of a physiological index of cognitive workload, when the task is not performed is a very constrained laboratory setting, but embedded in a more realistic and complex scenario. The expected increase of the frontal theta oscillation was not observed, and the power in the parietal alpha did not decrease as found in most workload studies, but it showed the contrary effect. The alpha effect is consistent with the literature on non-visual tasks. The common hypothesis for this ambiguity in the alpha rhythm is that the task-irrelevant visual brain region is actively inhibited in order to focus resources to the relevant non-visual processing tasks. One participant that showed a parieto-occipital alpha decrease might have had a visual strategy to memorize the sequence of numbers, albeit they have been presented auditorily.

Classification of workload levels in the complex *bow-to-bow* scenario is in general successful. Transferring the classifier between the two phases 1 and 3 does not degrade the performance appreciably. The fact that classification in the realistic *bow-to-bow* task worked less good compared to the *2-back* task requires consideration. As found in the literature on electrophysiological correlates of workload, there are two opposing effect concerning the modulation of the alpha rhythm. Tasks in the visual modality are found to decrease alpha activity, while workload in non-vusial modalities were partly found to increase alpha activity (as in our *2-back* paradigm). In the complex *bow-to-bow* scenario, these effects may be in conflict. Retrieving expertise about the maneuvering can be expected to be mainly non-visual. Nevertheless, the control of the boat does not allow a rigorous inhibition of visual processing (that would be reflected by strong alpha increase) as it requires synchronized visual processing, in particular as the weather conditions were challenging in during the high workload condition. This conflict can be assume to leading to a much weaker effect of cognitive workload on alpha power, an issue that would be well worth deeper investigation.

Another interesting point in the view of applicability is the fact that the complex concept workload encompasses different factors, two of which are *activation* and *resources*, as dicsussed in Sec. 3.1. Therefore, a high output of the workload monitor could indicate a strong activation in the sense of an effective focussing of the task at hand (thereby inhibiting task-irrelevant processing). Accordingly, an interpretation of the participant being at the limit of her/his resources might not be adequat.

7 Outlook

As a continuation of this project, we will investigate the descrimination of workload levels based on respiration data as well as the combination of signals from peripheral physiology and EEG. This will include respiration, heart rate (data provided by MARIN) and skin conductance (if data is provided by Phillips).

For the critical assessment of the current study on workload in a maritime manoevering task and for the interpretation in the view of applicability, we highlight the following points:

- There is a high variability in workload detection between participants. This has to be kept in mind for the target application.
- The current analysis operated on windows of 60 s duration. With shorter windows, the performance can be expected to degrade. This means that the workload monitor has some delay in the response.
- Transfer from the *2-back* to the *bow-to-bow* task was not possible. This means that the workload monitor needs to be calibrated with an actual maneuvering task in the simulator.
- The transfer between phases 1 and 3 (both *bow-to-bow* tasks) was well possible. Therefore, the workload monitor can be expected to be stable over some hours. However, this study did not investigate the transfer between sessions performed at different days. From experience with other BCI application, it can be assumed that at least some kind of recalibration is required.

As points of further investigation in future projects, we envision the following:

- How meaningful is the graded output of the workload indicator?
- Investigate why theta increase was not found in the *2-back* task. Is it due to the 'background' manoevering task?
- How is the alpha rhythm affected by cognitive workload in a dual visual and auditory task – do the effects found in separate studies of decreased in increase alpha power cancel out? Do we find other effects?
- Is the transfer of a workload classifier possible between days? What kind of recalibration is required to keep classification performance at a good level?
- Can we disentangle the contribution of *activation* and *resources* in the complex concept of cognitive workload.

References

[1] Anthony J. Bell and Terrence J. Sejnowski. An information-maximization approach to blind separation and blind deconvolution. *Neural Comput*, 7(6):1129–1159, 1995.

[2] Gilles Blanchard and Benjamin Blankertz. BCI competition 2003 – data set IIa: Spatial patterns of self-controlled brain rhythm modulations. *IEEE Trans Biomed Eng*, 51(6):1062–1066, 2004.

[3] Benjamin Blankertz, Michael Tangermann, Carmen Vidaurre, Siamac Fazli, Claudia Sannelli, Stefan Haufe, Cecilia Maeder, Lenny E Ramsey, Irene Sturm, Gabriel Curio, and Klaus-Robert Müller. The Berlin Brain-Computer Interface: Non-medical uses of BCI technology. *Front Neuroscience*, 4:198, 2010.

[4] Benjamin Blankertz, Ryota Tomioka, Steven Lemm, Motoaki Kawanabe, and Klaus-Robert Müller. Optimizing spatial filters for robust EEG single-trial analysis. *IEEE Signal Process Mag*, 25(1):41–56, 2008.

[5] Pierre Comon. Independent component analysis, a new concept? *Signal Processing*, 36(3):287–314, 1994.

[6] J. H. Friedman. Regularized discriminant analysis. *J Amer Statist Assoc*, 84(405):165–175, 1989.

[7] Keinosuke Fukunaga. *Introduction to statistical pattern recognition.* Academic Press, Boston, 2nd edition edition, 1990.

[8] David Galin, Jack Johnstone, and Jeannine Herron. Effects of task difficulty on eeg measures of cerebral engagement. *Neuropsychologia*, 16(4):461–472, 1978.

[9] A Gevins, H Leong, R Du, M E Smith, J Le, D DuRousseau, J Zhang, and J Libove. Towards measurement of brain function in operational environments. *Biological Psychology*, 40(1-2):169–186, 1995.

[10] Alan Gevins and Michael E. Smith. Neurophysiological measures of cognitive workload during human-computer interaction. *Theoretical Issues in Ergonomics Science*, 4(1-2):113–131, 2003.

[11] Alan Gevins, Michael E. Smith, Harrison Leong, Linda McEvoy, Susan Whitfield, Robert Du, and Georgia Rush. Monitoring working memory load during computer-based tasks with EEG pattern recognition methods. *Hum Factors*, 40(1):79–91, 1998.

[12] Alexander Gundel and Glenn F Wilson. Topographical changes in the ongoing eeg related to the difficulty of mental tasks. *Brain Topogr*, 5(1):17–25, 1992.

[13] A. Holm, K. Lukander, J. Korpela, M. Sallinen, and K. M. Muller. Estimating brain load from the EEG. *ScientificWorldJournal*, 9:639–651, 2009.

[14] A. Hyvärinen, J. Karhunen, and E. Oja. *Independent Component Analysis*. Wiley, 2001.

[15] W K Kirchner. Age differences in short-term retention of rapidly changing information. *Journal of Experimental Psychology*, 55:352–358, 1958.

[16] W Klimesch, M Doppelmayr, J Schwaiger, P Auinger, and Th Winkler. Paradoxical'alpha synchronization in a memory task. *Cogn Brain Res*, 7(4):493–501, 1999.

[17] Jens Kohlmorgen, Guido Dornhege, Mikio Braun, Benjamin Blankertz, Klaus-Robert Müller, Gabriel Curio, Konrad Hagemann, Andreas Bruns, Michael Schrauf, and Wilhelm Kincses. Improving human performance in a real operating environment through real-time mental workload detection. In Guido Dornhege, Jose del R. Millán, Thilo Hinterberger, Dennis McFarland, and Klaus-Robert Müller, editors, *Toward Brain-Computer Interfacing*, pages 409–422. MIT press, Cambridge, MA, 2007.

[18] Albert Kok. Event-related-potential (erp) reflections of mental resources: a review and synthesis. *Biol Psychol*, 45(1):19–56, 1997.

[19] Arthur F Kramer. Physiological metrics of mental workload: A review of recent progress. In D. L. Damos, editor, *Multiple-task performance*, pages 279–328. Taylor & Francis, 1991.

[20] H Legewie, O Simonova, and OD Creutzfeldt. Eeg changes during performance of various tasks under open-and closed-eyed conditions. *Electroencephalogr Clin Neurophysiol*, 27(5):470–479, 1969.

[21] Steven Lemm, Benjamin Blankertz, Thorsten Dickhaus, and Klaus-Robert Müller. Introduction to machine learning for brain imaging. *Neuroimage*, 56:387–399, 2011.

[22] Omkar N Markand. Alpha rhythms. *J Clin Neurophysiol*, 7(2):163–190, 1990.

[23] R. Parasuraman and G.F. Wilson. Putting the brain to work: Neuroergonomics past, present, and future. *Hum Factors*, 50(3):468, 2008.

[24] L.C. Parra, C. Christoforou, A.D. Gerson, M. Dyrholm, An Luo, M. Wagner, M.G. Philiastides, and P. Sajda. Spatiotemporal linear decoding of brain state. *IEEE Signal Process Mag*, 25(1):107–115, 2008.

[25] John Polich. Task difficulty, probability, and inter-stimulus interval as determinants of p300 from auditory stimuli. *Electroencephalography and Clinical Neurophysiology/Evoked Potentials Section*, 68(4):311 – 320, 1987.

[26] Alan T Pope, Edward H Bogart, and Debbie S Bartolome. Biocybernetic system evaluates indices of operator engagement in automated task. *Biol Psychol*, 40(1):187–195, 1995.

[27] L. J. Prinzel, F. G. Freeman, M. W. Scerbo, P. J. Mikulka, and A. T. Pope. Effects of a psychophysiological system for adaptive automation on performance, workload, and the event-related potential P300 component. *Hum Factors*, 45:601–613, 2003.

[28] H. Ramoser, J. Müller-Gerking, and G. Pfurtscheller. Optimal spatial filtering of single trial EEG during imagined hand movement. *IEEE Trans Rehabil Eng*, 8(4):441–446, 2000.

[29] M. E. Smith, A. Gevins, H. Brown, A. Karnik, R. Du, and A. S. Gevins. Monitoring task loading with multivariate EEG measures during complex forms of human-computer interaction. *Hum Factors*, 43:366–380, 2001.

[30] Carmen Vidaurre, Nicole Krämer, Benjamin Blankertz, and Alois Schlögl. Time domain parameters as a feature for EEG-based brain computer interfaces. *Neural Networks*, 22:1313–1319, 2009.

[31] Irene Winkler, Stefan Haufe, and Michael Tangermann. Automatic classification of artifactual ICA-components for artifact removal in EEG signals. *Behav Brain Funct*, 7(1):30, 2011.

A Neural Correlates of Workload in Selected Participants – 2-Back Task

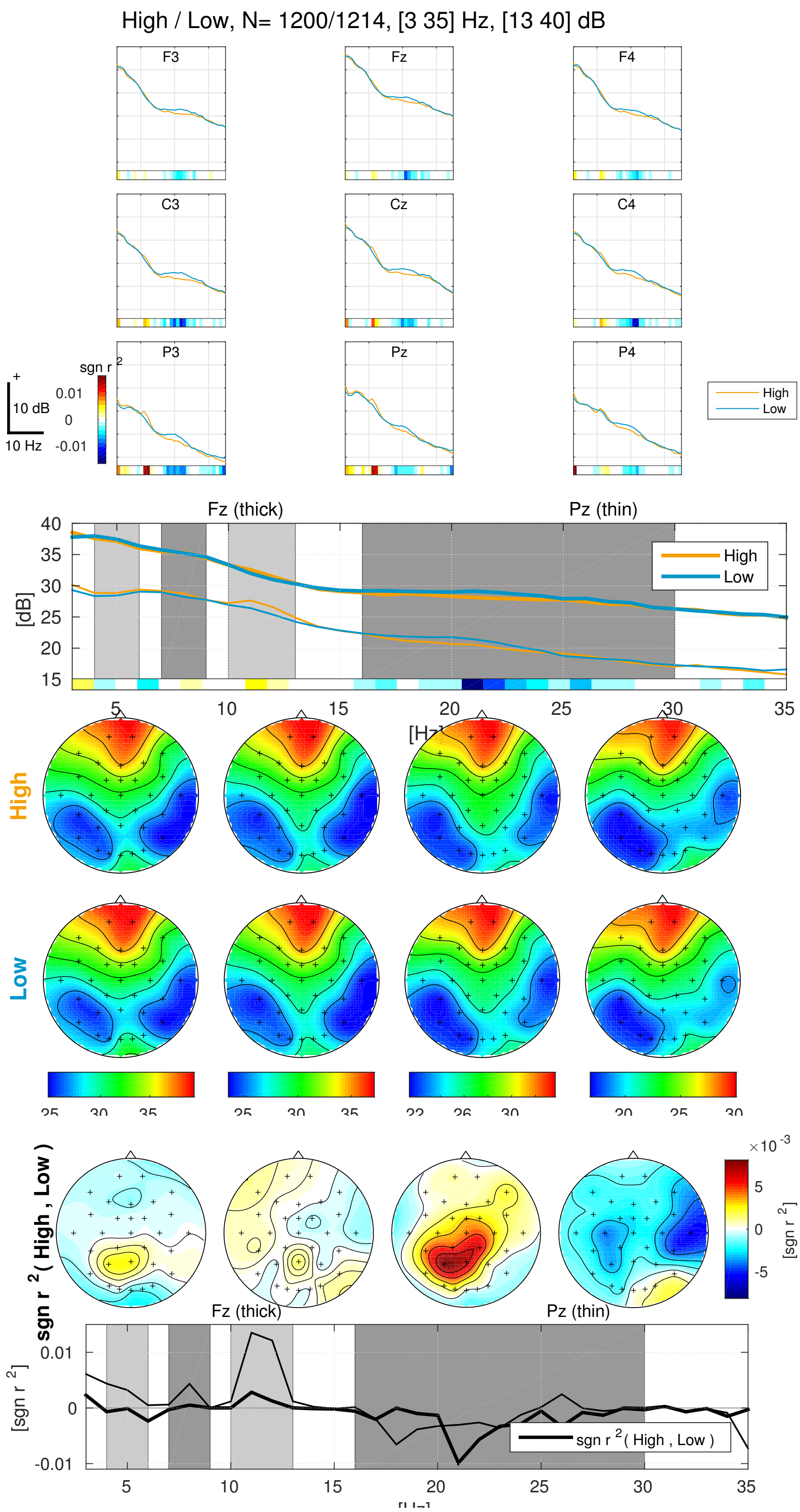

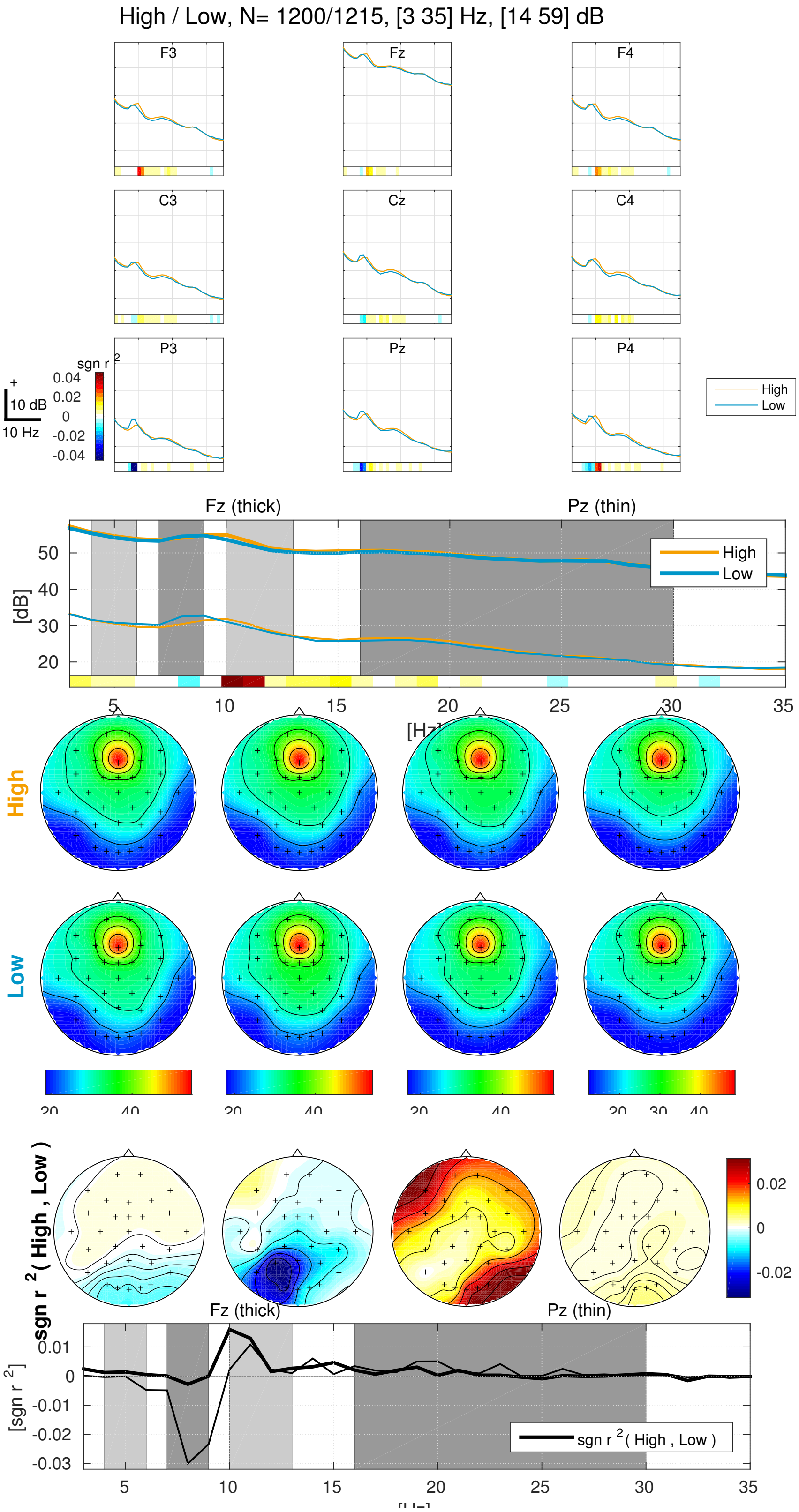
High / Low, N= 1200/1215, [3 35] Hz, [14 59] dB
F3
Fz
F4
C3
Cz
C4
P3
Pz
P4
sgn r 2
10 dB
10 Hz
High
Low
Fz (thick)
Pz (thin)
[dB]
[Hz]
sgn r 2 (High , Low)
[sgn r 2]

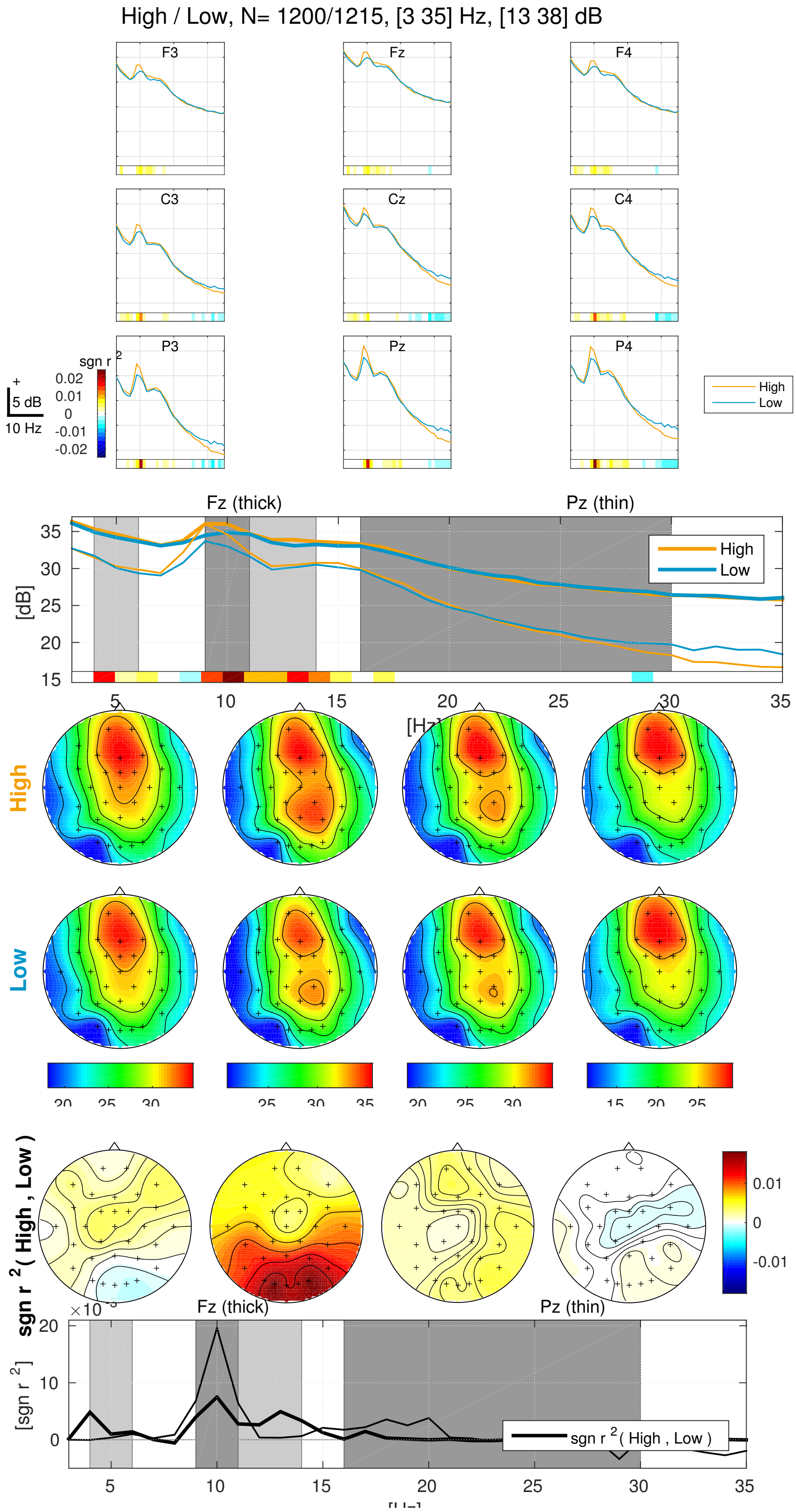
High / Low, N= 1200/1215, [3 35] Hz, [13 38] dB
F3
Fz
F4
C3
Cz
C4
P3
Pz
P4
sgn r 2
0.02
0.01
0
-0.01
-0.02
5 dB
10 Hz
High
Low
Fz (thick)
Pz (thin)
[dB]
[Hz]
High
Low
sgn r 2(High , Low)
0.01
0
-0.01
×10 -3
[sgn r 2]
sgn r 2(High , Low)

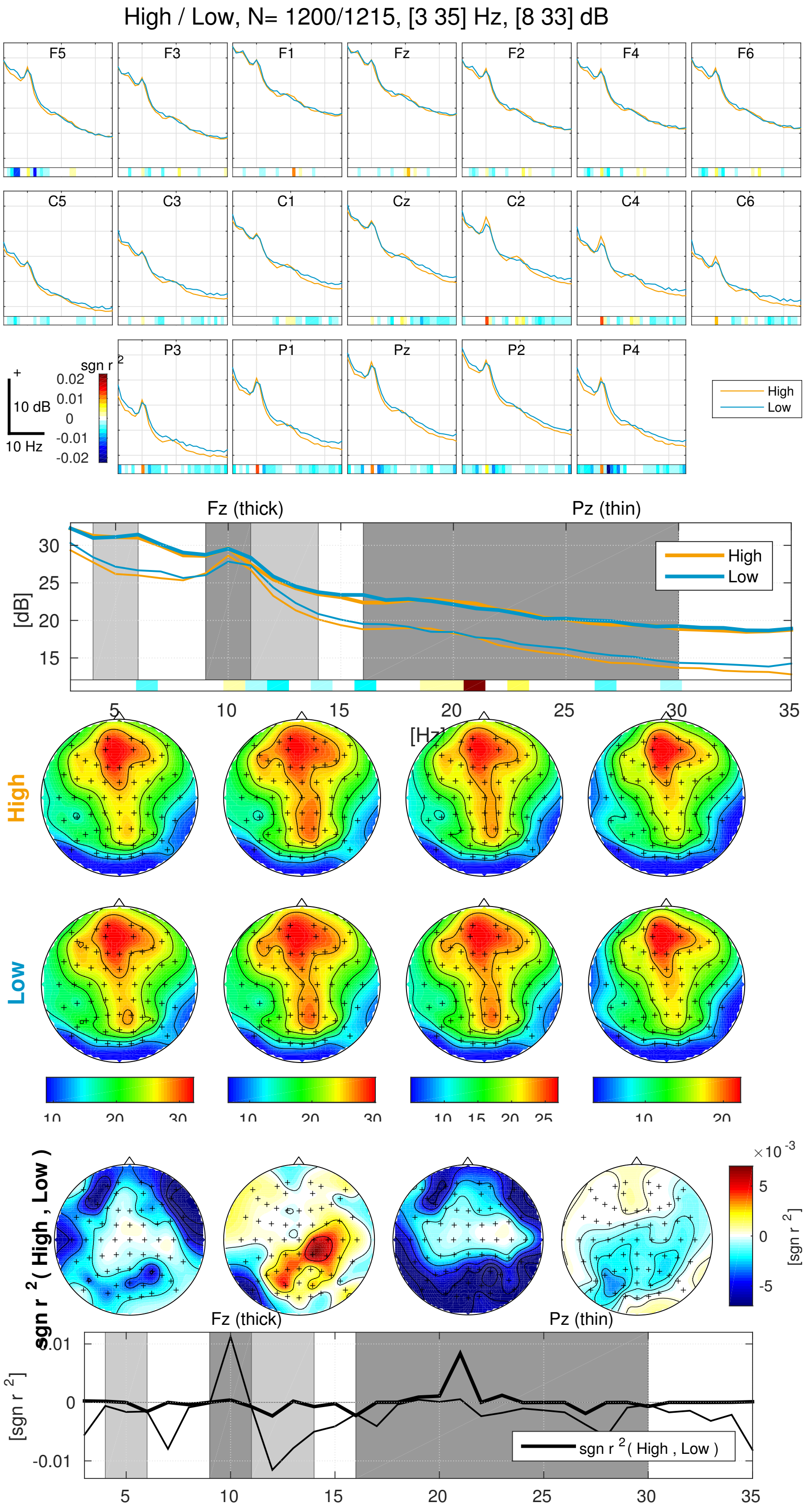
High / Low, N= 1200/1215, [3 35] Hz, [8 33] dB
F5
F3
F1
Fz
F2
F4
F6
C5
C3
C1
Cz
C2
C4
C6
P3
P1
Pz
P2
P4
sgn r 2
10 dB
10 Hz
High
Low
Fz (thick)
Pz (thin)
[dB]
[Hz]
High
Low
sgn r 2 (High , Low)
[sgn r 2]
sgn r 2 (High , Low)

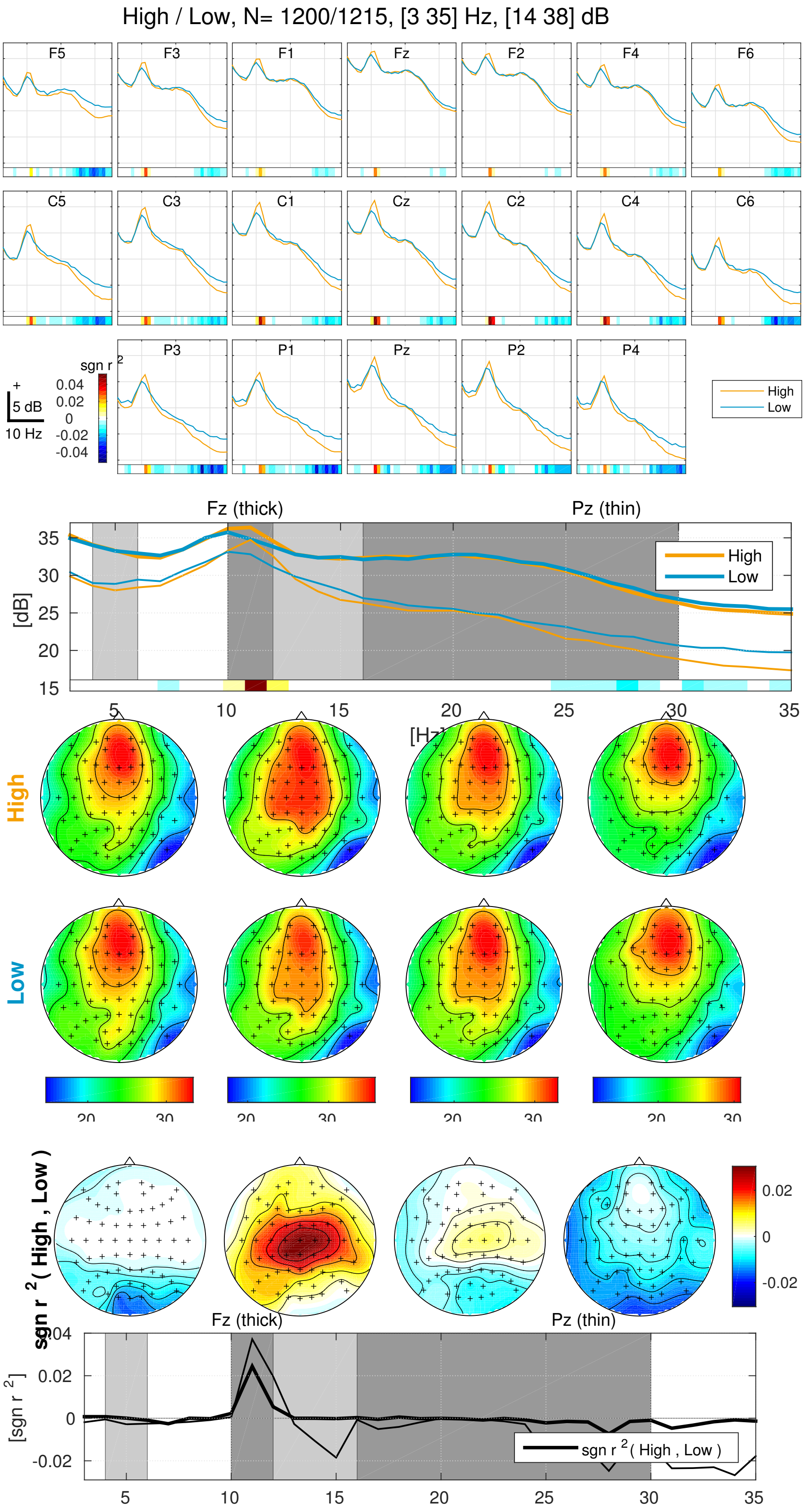

High / Low, N= 1200/1215, [3 35] Hz, [14 38] dB
F5 F3 F1 Fz F2 F4 F6
C5 C3 C1 Cz C2 C4 C6
P3 P1 Pz P2 P4
sgn r 2
0.04 0.02 0 -0.02 -0.04
5 dB
10 Hz
High
Low
Fz (thick)
Pz (thin)
[dB]
[Hz]
High
Low
sgn r 2 (High , Low)
0.02 0 -0.02
[sgn r 2]

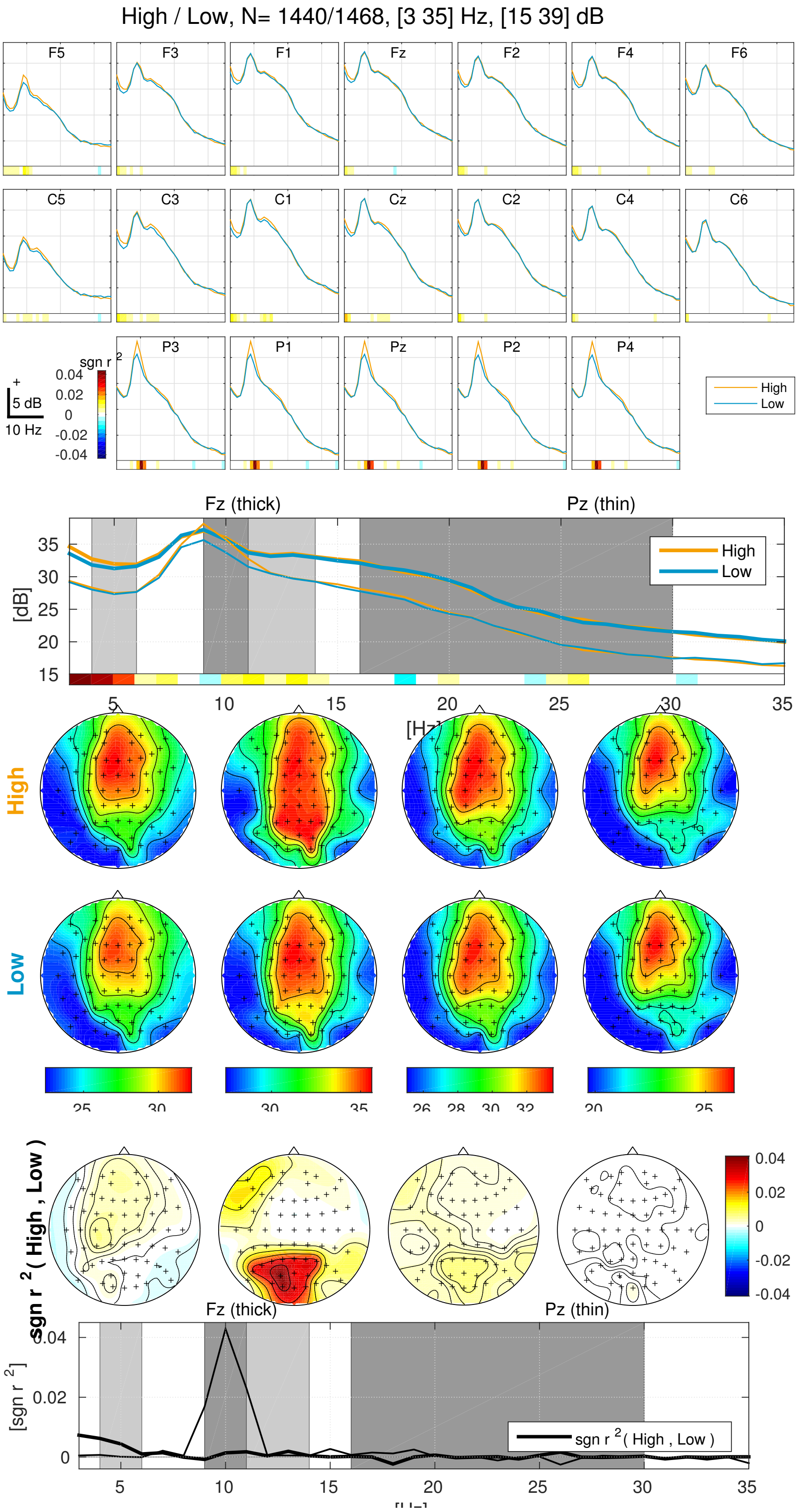

High / Low, N= 1440/1468, [3 35] Hz, [15 39] dB
F5
F3
F1
Fz
F2
F4
F6
C5
C3
C1
Cz
C2
C4
C6
P3
P1
Pz
P2
P4
sgn r 2
0.04
0.02
0
-0.02
-0.04
5 dB
10 Hz
High
Low
Fz (thick)
Pz (thin)
[dB]
[Hz]
High
Low
sgn r 2(High , Low)
[sgn r 2]
sgn r 2(High , Low)

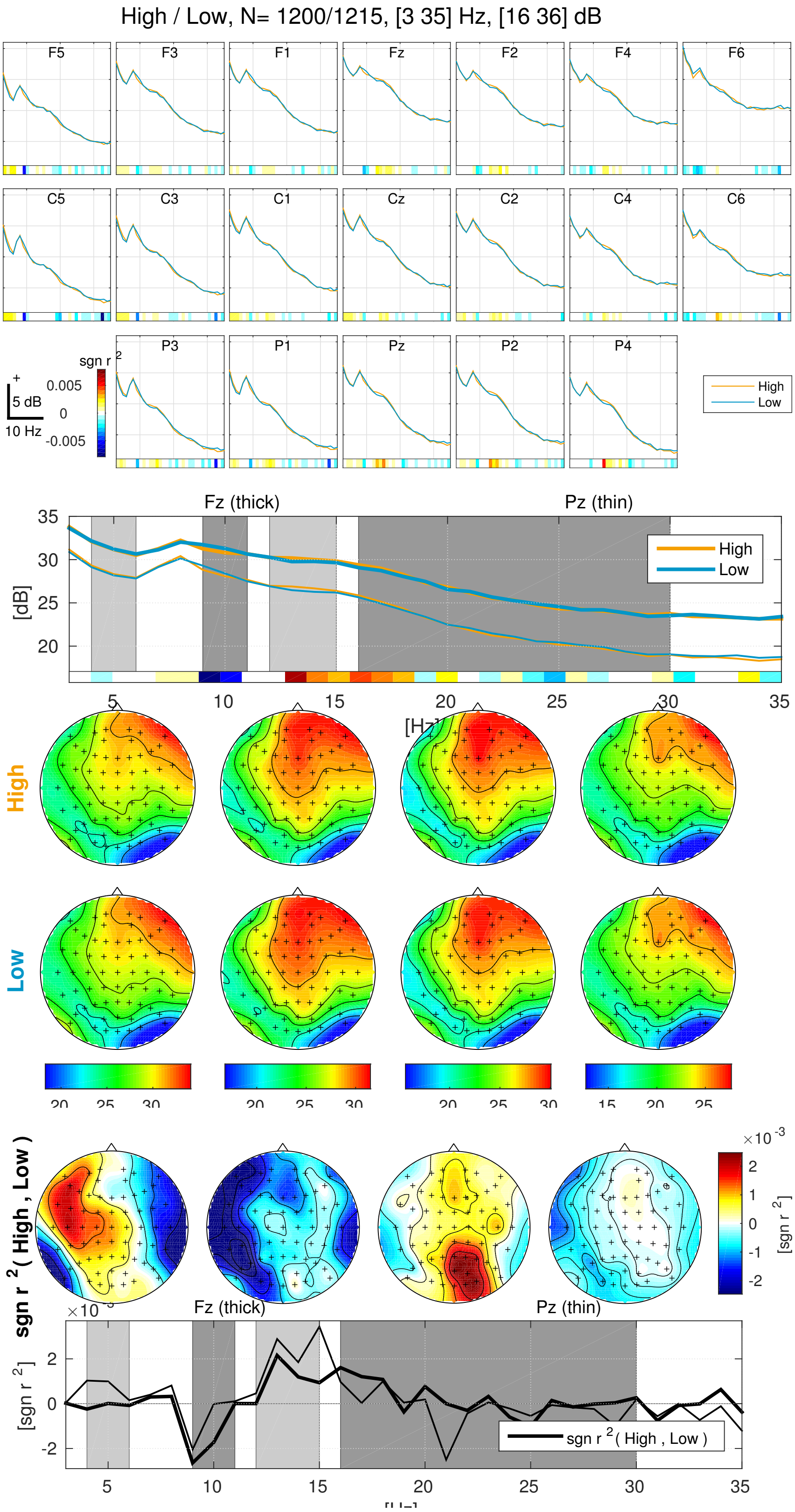

High / Low, N= 1200/1215, [3 35] Hz, [16 36] dB
F5
F3
F1
Fz
F2
F4
F6
C5
C3
C1
Cz
C2
C4
C6
P3
P1
Pz
P2
P4
5 dB
10 Hz
0.005
0
-0.005
High
Low
Fz (thick)
Pz (thin)
[dB]
[Hz]
High
Low
sgn r 2(High , Low)
[sgn r 2]

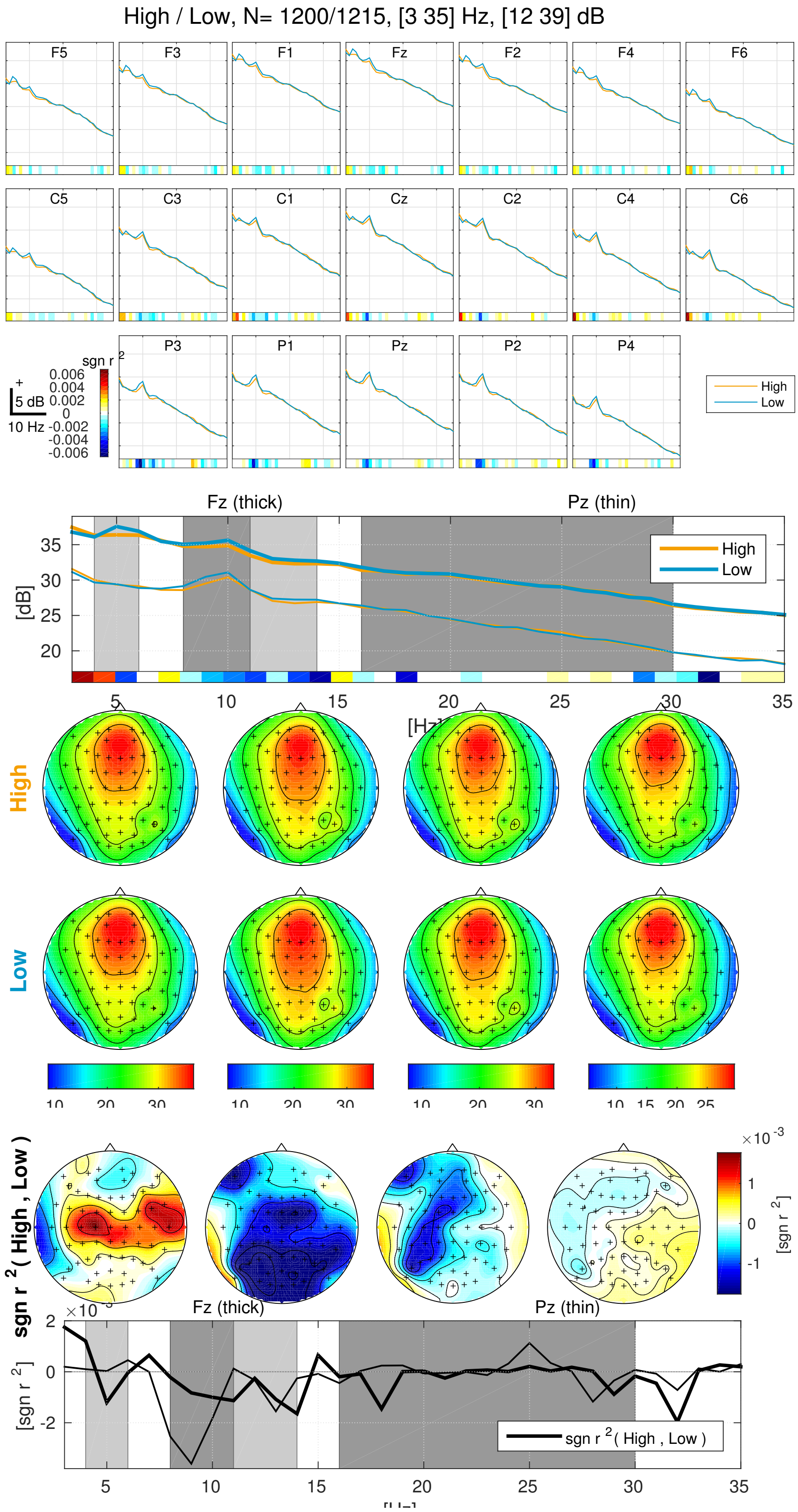
High / Low, N= 1200/1215, [3 35] Hz, [12 39] dB
F5
F3
F1
Fz
F2
F4
F6
C5
C3
C1
Cz
C2
C4
C6
P3
P1
Pz
P2
P4
sgn r 2
5 dB
10 Hz
High
Low
Fz (thick)
Pz (thin)
[dB]
[Hz]
High
Low
sgn r 2 (High , Low)
[sgn r 2]
sgn r 2 (High , Low)

B Neural Correlates of Workload in Selected Participants – Bow-to-Bow Task

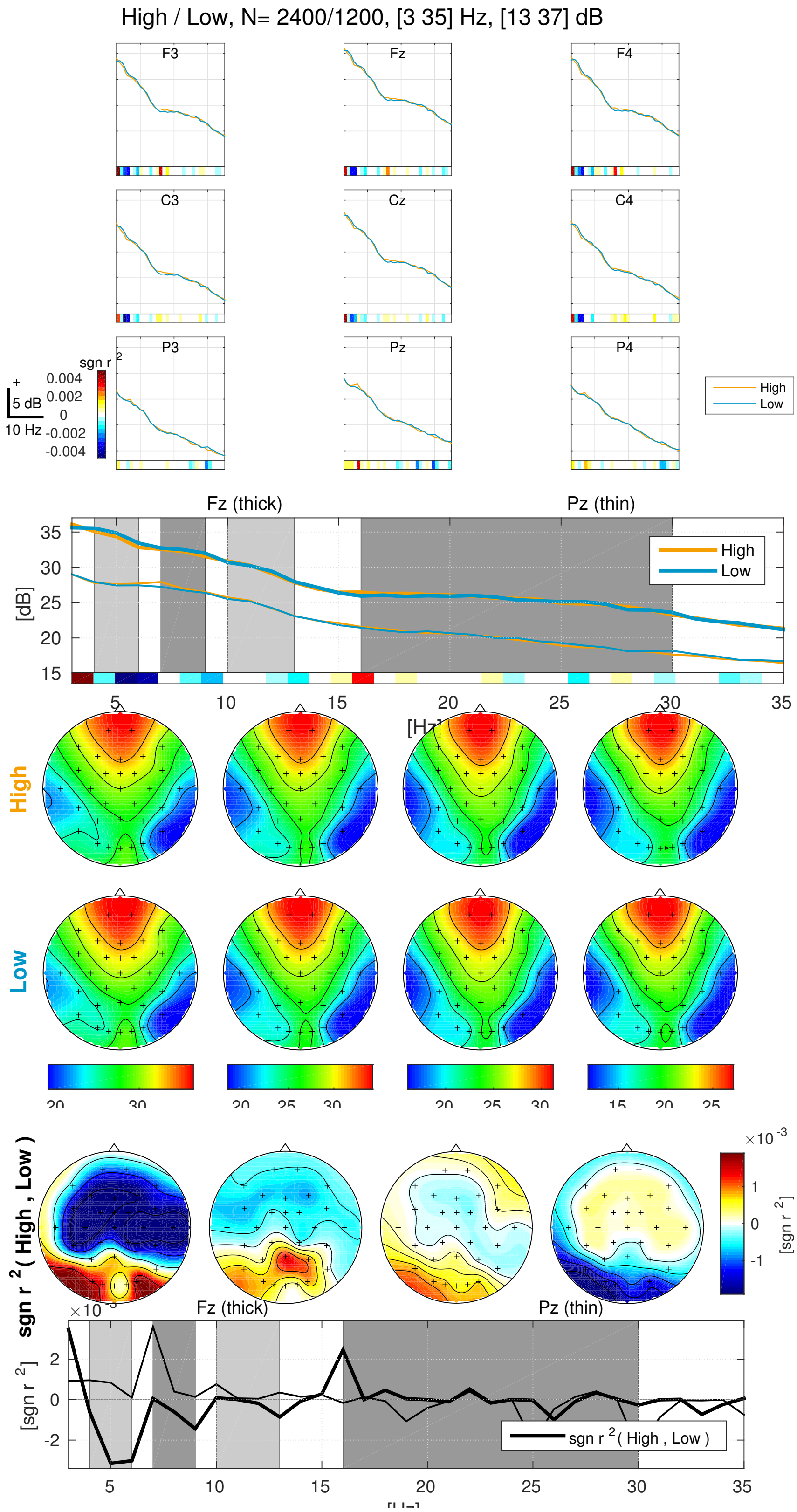

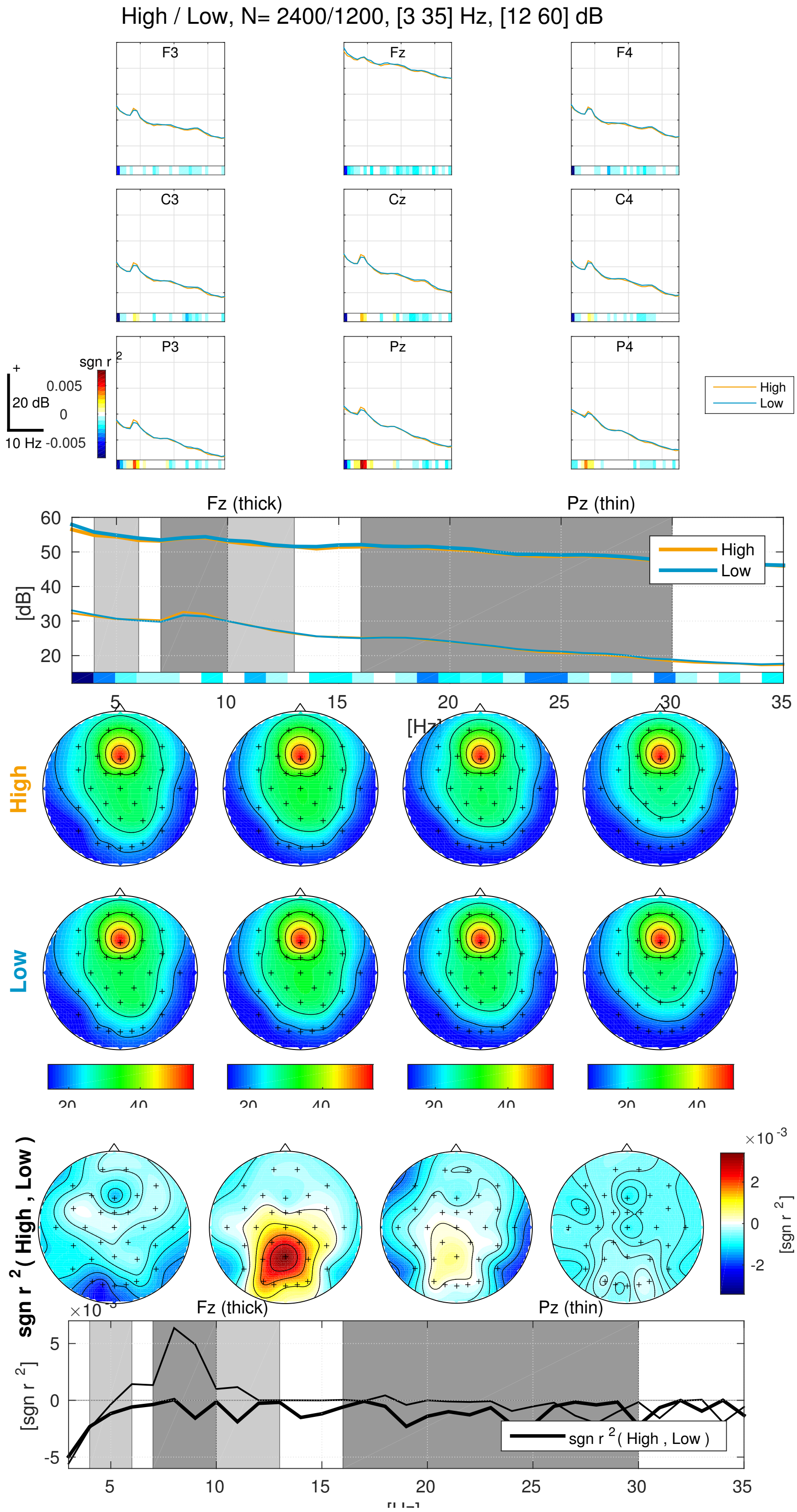
High / Low, N= 2400/1200, [3 35] Hz, [12 60] dB
F3
Fz
F4
C3
Cz
C4
P3
Pz
P4
sgn r 2
0.005
0
-0.005
20 dB
10 Hz
High
Low
Fz (thick)
Pz (thin)
[dB]
[Hz]
High
Low
sgn r 2(High , Low)
[sgn r 2]
×10 -3
sgn r 2(High , Low)

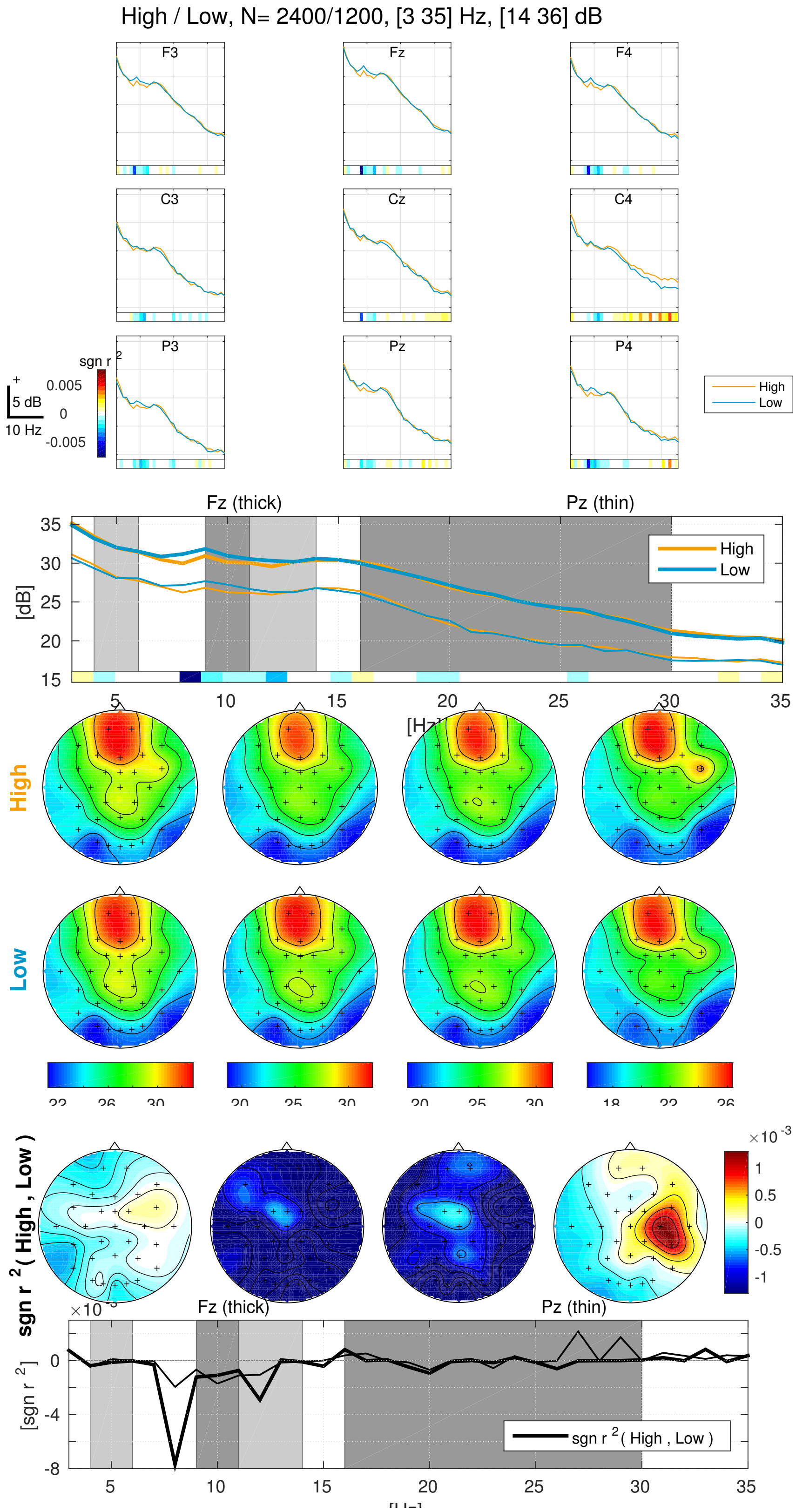

High / Low, N= 2400/1200, [3 35] Hz, [14 36] dB
F3
Fz
F4
C3
Cz
C4
P3
Pz
P4
sgn r 2
0.005
0
-0.005
5 dB
10 Hz
High
Low
Fz (thick)
Pz (thin)
[dB]
[Hz]
High
Low
sgn r 2(High , Low)
[sgn r 2]

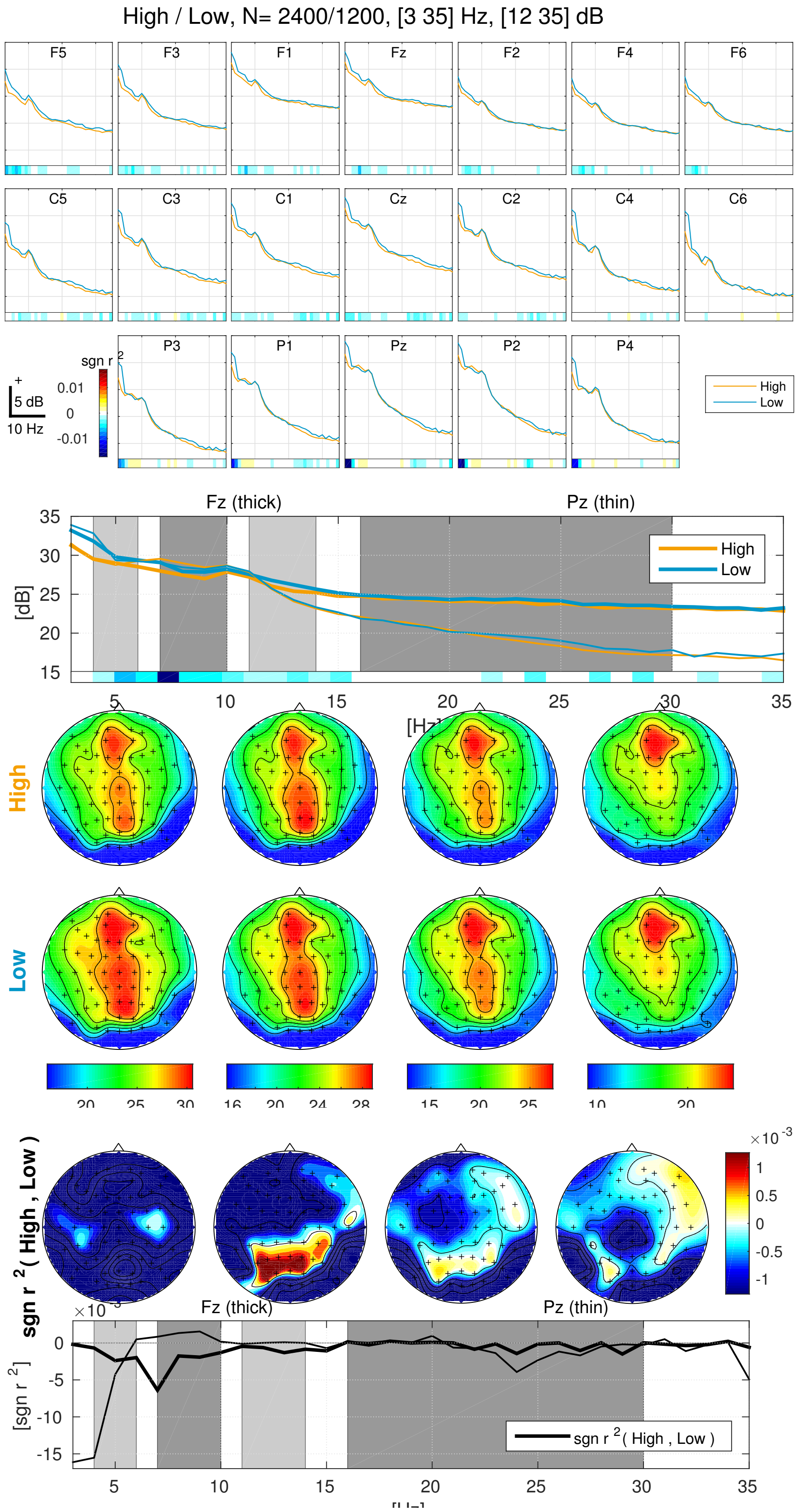

High / Low, N= 2400/1200, [3 35] Hz, [12 35] dB
F5
F3
F1
Fz
F2
F4
F6
C5
C3
C1
Cz
C2
C4
C6
P3
P1
Pz
P2
P4
sgn r 2
5 dB
10 Hz
0.01
0
-0.01
High
Low
Fz (thick)
Pz (thin)
[dB]
High
Low
sgn r 2(High , Low)
[sgn r 2]
sgn r 2(High , Low)

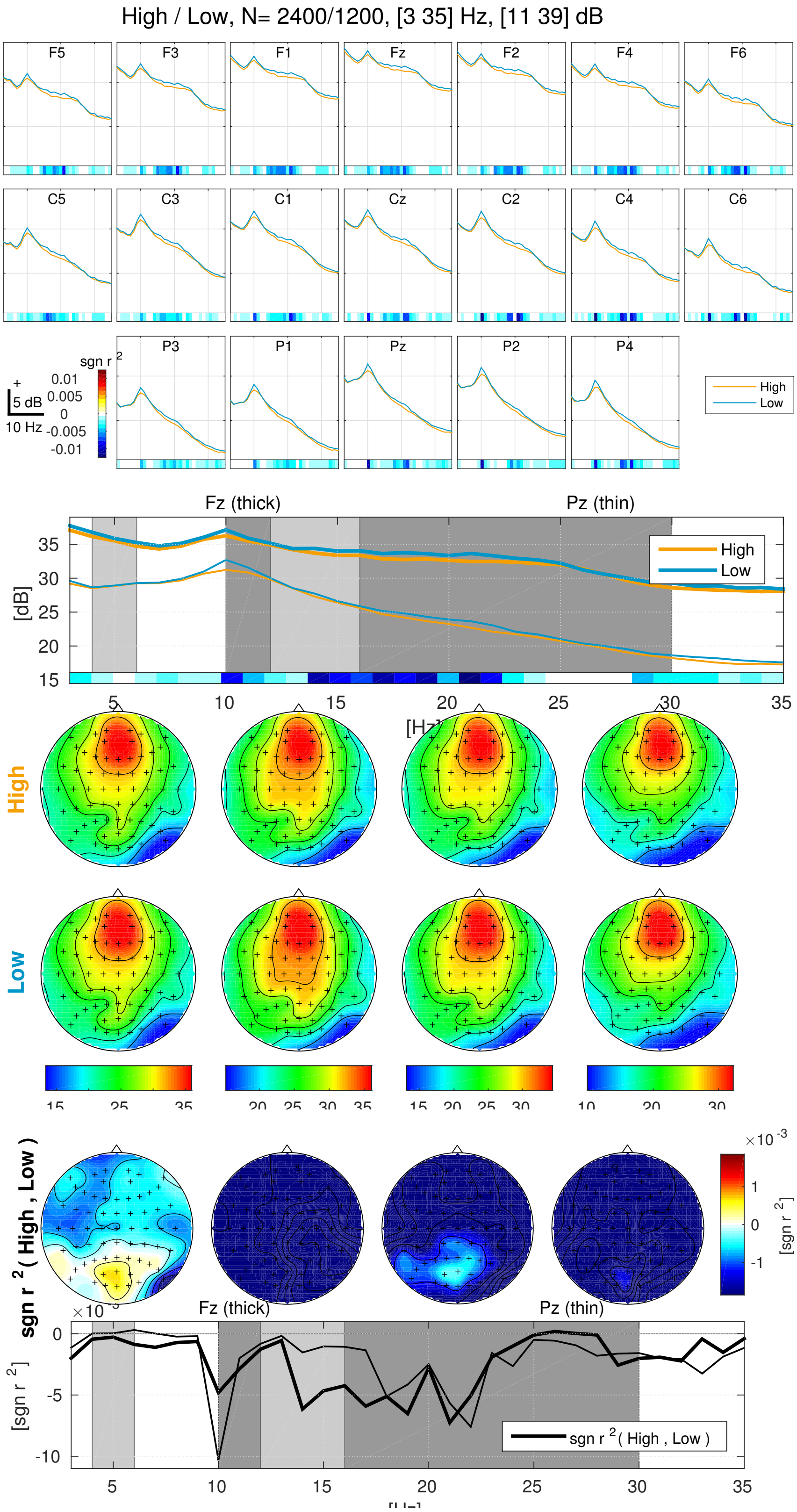
High / Low, N= 2400/1200, [3 35] Hz, [11 39] dB
F5
F3
F1
Fz
F2
F4
F6
C5
C3
C1
Cz
C2
C4
C6
P3
P1
Pz
P2
P4
sgn r 2
5 dB
10 Hz
0.01
0.005
0
-0.005
-0.01
High
Low
Fz (thick)
Pz (thin)
[dB]
[Hz]
High
Low
×10 -3
[sgn r 2]
sgn r 2 (High , Low)
sgn r 2 (High , Low)

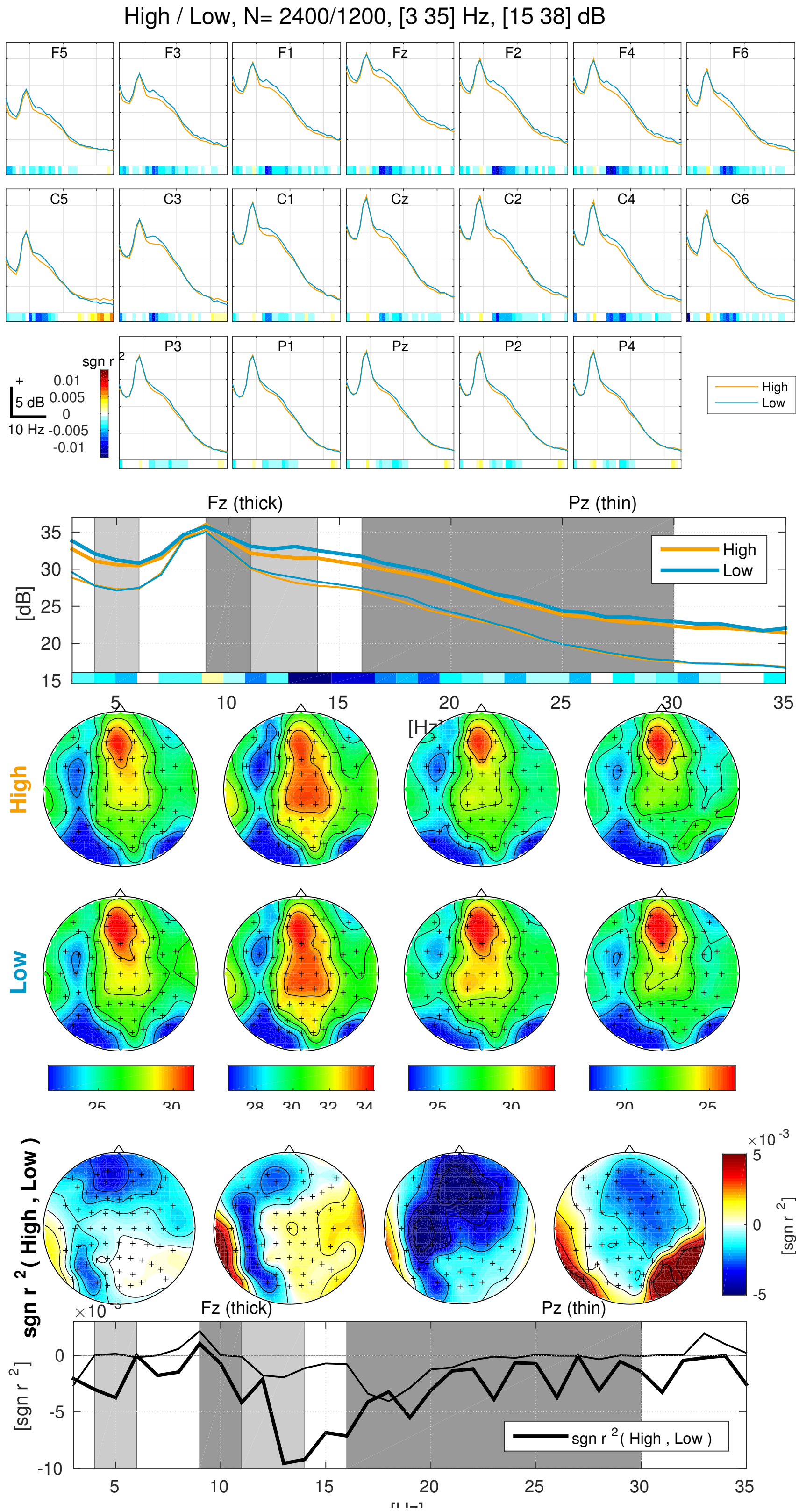

High / Low, N= 2400/1200, [3 35] Hz, [15 38] dB
F5
F3
F1
Fz
F2
F4
F6
C5
C3
C1
Cz
C2
C4
C6
P3
P1
Pz
P2
P4
sgn r 2
+
5 dB
10 Hz
0.01
0.005
0
-0.005
-0.01
High
Low
Fz (thick)
Pz (thin)
[dB]
[Hz]
High
Low
sgn r 2 (High , Low)
×10 -3
[sgn r 2]
sgn r 2 (High , Low)

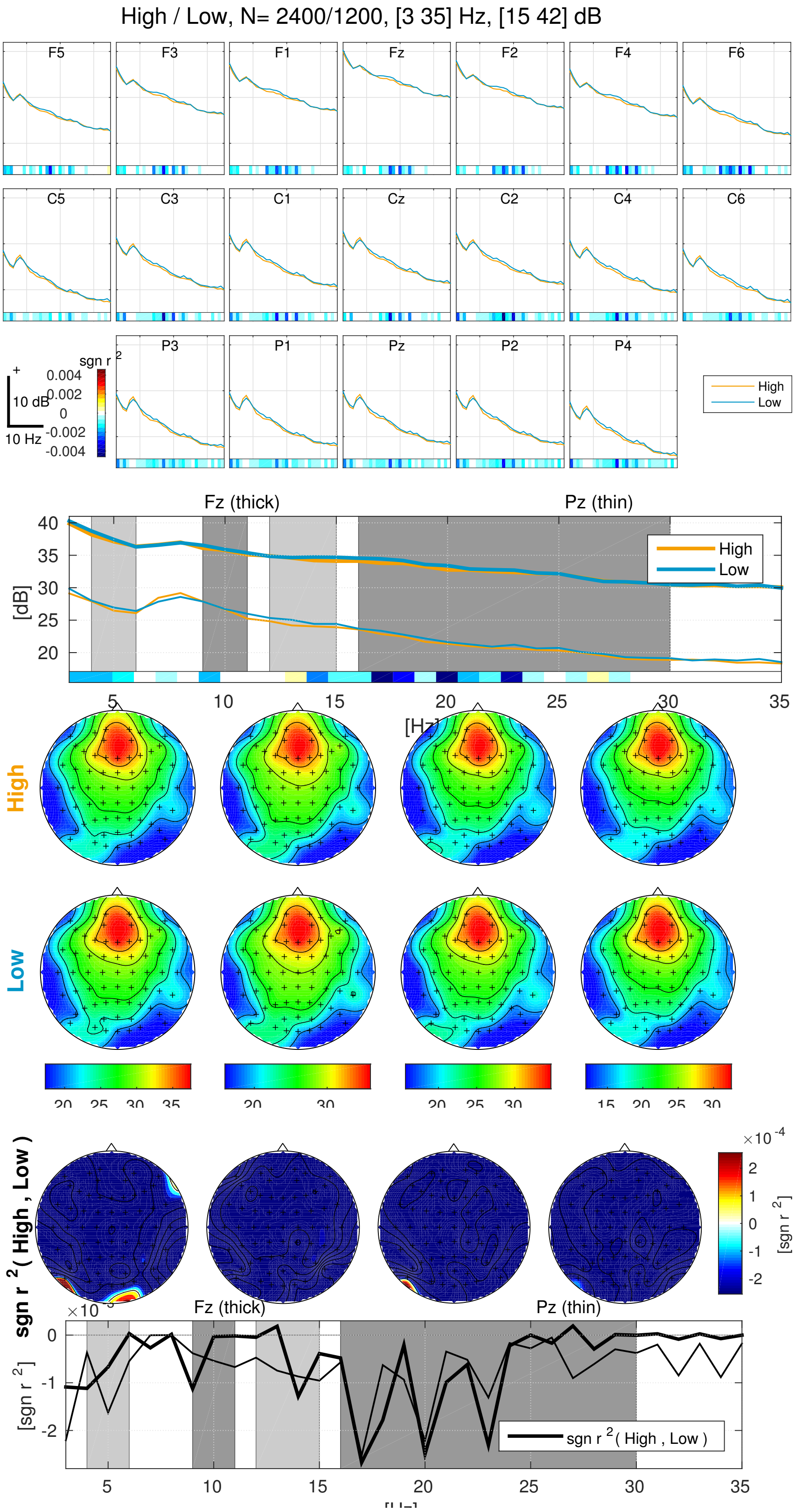
High / Low, N= 2400/1200, [3 35] Hz, [15 42] dB
F5
F3
F1
Fz
F2
F4
F6
C5
C3
C1
Cz
C2
C4
C6
P3
P1
Pz
P2
P4
10 dB
10 Hz
sgn r 2
High
Low
Fz (thick)
Pz (thin)
[dB]
[Hz]
High
Low
sgn r 2(High , Low)
[sgn r 2]
sgn r 2(High , Low)

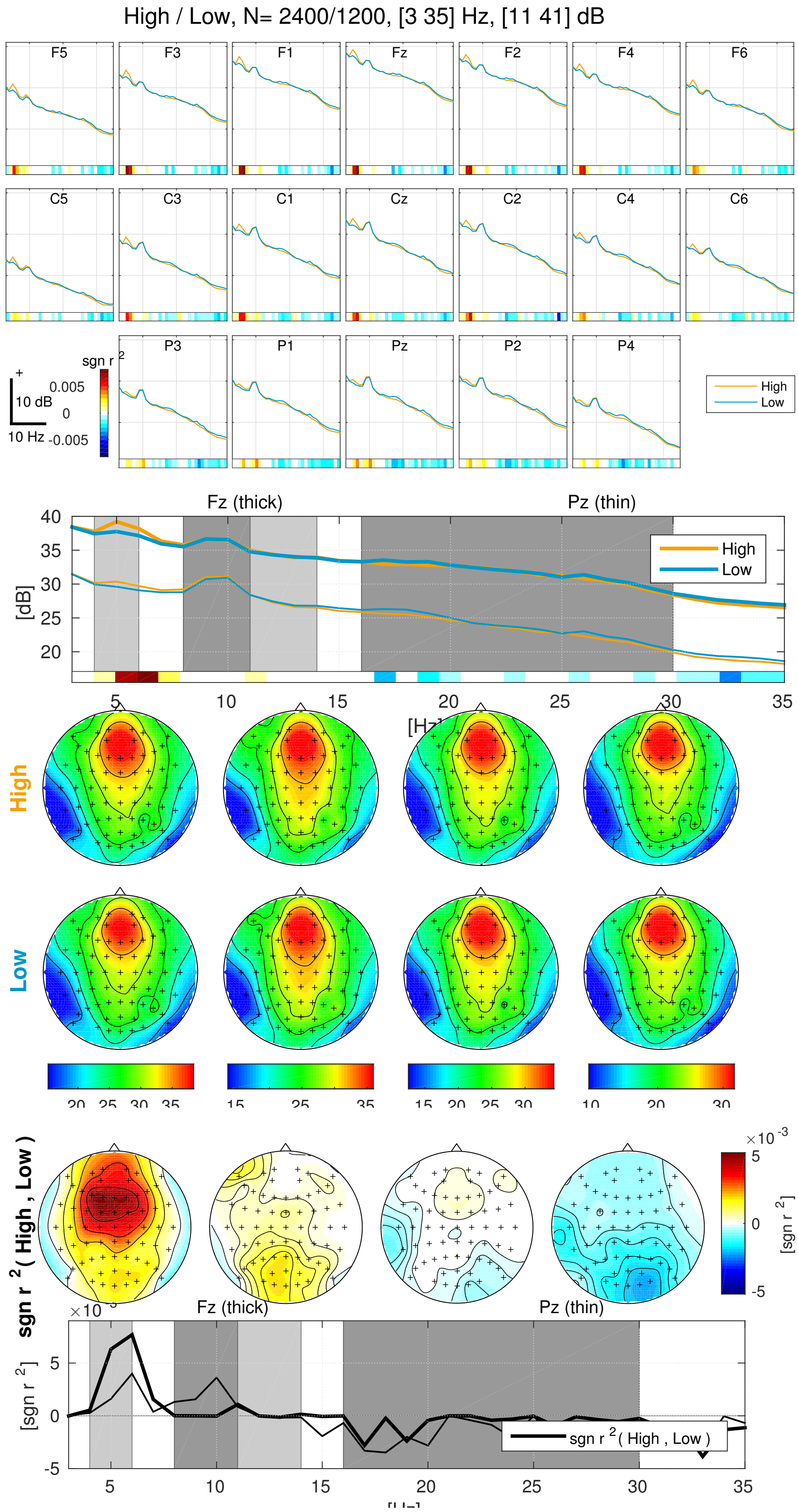
High / Low, N= 2400/1200, [3 35] Hz, [11 41] dB
F5
F3
F1
Fz
F2
F4
F6
C5
C3
C1
Cz
C2
C4
C6
P3
P1
Pz
P2
P4
sgn r 2
0.005
0
-0.005
10 dB
10 Hz
High
Low
Fz (thick)
Pz (thin)
[dB]
[Hz]
High
Low
sgn r 2(High , Low)
[sgn r 2]
×10 -3
sgn r 2(High , Low)